



MAGNETIZED PLASMA WITH FERRITE GRAINS AS
TUNABLE ANISOTROPIC LEFT HANDED MEDIA

By

Kassu Shiferaw

A GRADUATE THESIS
SUBMITTED IN PARTIAL FULFILLMENT OF THE
REQUIREMENTS FOR THE DEGREE OF
MASTER OF SCIENCE
AT
ADDIS ABABA UNIVERSITY

ADDIS ABABA, ETHIOPIA

AUGUST 2016

ADDIS ABABA UNIVERSITY
DEPARTMENT OF
PHYSICS

The undersigned hereby certify that they have read and recommend to the School of Graduate Studies for acceptance a thesis entitled “**Magnetized Plasma with Ferrite Grains as Tunable Anisotropic Left Handed Media**” by **Kassu Shiferaw** in partial fulfillment of the requirements for the degree of **Master of Science**.

Dated: August 2016

Examiners:

Dr. Teshome Senbeta

Dr. Deribe Hirpo

Supervisor:

Dr. Belayneh Mesfin

ADDIS ABABA UNIVERSITY

Date: **August 2016**

Author: **Kassu Shiferaw**

Title: **Magnetized Plasma with Ferrite Grains as Tunable
Anisotropic Left Handed Media**

Department: **Physics**

Degree: **M.Sc.** Convocation: **August** Year: **2016**

Permission is herewith granted to Addis Ababa University to circulate and to have copied for non-commercial purposes, at its discretion, the above title upon the request of individuals or institutions.

Signature of Author

THE AUTHOR RESERVES OTHER PUBLICATION RIGHTS, AND NEITHER THE THESIS NOR EXTENSIVE EXTRACTS FROM IT MAY BE PRINTED OR OTHERWISE REPRODUCED WITHOUT THE AUTHOR'S WRITTEN PERMISSION.

THE AUTHOR ATTESTS THAT PERMISSION HAS BEEN OBTAINED FOR THE USE OF ANY COPYRIGHTED MATERIAL APPEARING IN THIS THESIS (OTHER THAN BRIEF EXCERPTS REQUIRING ONLY PROPER ACKNOWLEDGEMENT IN SCHOLARLY WRITING) AND THAT ALL SUCH USE IS CLEARLY ACKNOWLEDGED.

Table of Contents

Table of Contents	iv
List of Tables	vi
List of Figures	vii
Abstract	x
Acknowledgements	xi
1 Introduction	1
2 Theoretical Background	6
2.1 Basic Concepts and Definitions	6
2.1.1 Maxwell's Equations and the Constitutive Relations	6
2.1.2 Phase Velocity, Group Velocity and Poynting Vector	9
2.2 Laws of Physics in NIMs	12
2.3 Metamaterials	14
2.3.1 Materials with Negative Permittivity	14
2.3.2 Materials with Negative Permeability	18
2.4 Materials with negative refractive index	20
3 Contemporary Ideas and New Frontiers in Search of Metamaterials	24
3.1 Chiral Materials	25
3.2 Anisotropic and Bianisotropic Media	27
4 Magnetized Plasma with Ferromagnetic Grains	30
4.1 Electromagnetic Waves in Magnetized Plasma	30
4.1.1 Electromagnetic wave parallel to \mathbf{B}	32
4.1.2 Electromagnetic wave perpendicular to \mathbf{B}	33

4.2	Electromagnetic Waves in MPFG	34
4.2.1	The permeability tensor	35
4.2.2	The dispersion relation	37
4.3	Phase velocity, group velocity and energy flow in MPFG	52
5	Conclusion	57
	Bibliography	58

List of Tables

4.1	The different ranges of frequencies where the MPFG is RHM, LHM or nontransparent when the wave is parallel.	44
4.2	The different ranges of frequencies where the MPFG is RHM, LHM or nontransparent when the wave is perpendicular.	52

List of Figures

1.1	Summary of MM results from RF to near optical frequencies. In the left column the frequency ranges in which each MM was demonstrated are depicted. The middle column shows a photo of the MM from each publication, and the third column shows some data detailing the MM response.[Adapted from [6]]	4
2.1	Material parameter space characterized by electric permittivity (ϵ) and magnetic permeability (μ).	8
2.2	Snell's law for positive ϵ and μ (path 1-2) and for negative ϵ and μ (path 1-3).	13
2.3	An array of nonmagnetic, infinitely long, thin metal wires behaves as a low frequency plasma for an electric field oriented along the wires. .	17
2.4	(Left) Split ring resonator. (Right) Split ring in flat two dimension. d is the separation between the rings.	19
2.5	(a) Diagram of a single split-ring resonator (SRR), $c = 50.25 \text{ mm}$, $d = 50.30 \text{ mm}$, $g = 50.46 \text{ mm}$, $w = 52.62 \text{ mm}$, and the SRR is square. (b) Each unit cell has six copper SRRs and two wire strips on thin fiberglass boards. The wire strips are 1 cm long, centered on the SRRs, and on the opposite side of the board from the SRRs. The angle between the fiberglass boards is 90° to make square unit cells with a lattice constant of 5.0 mm . [Extracted from [16]]	21

2.6	(a) The LHM sample consists of square copper split ring resonators and copper wire strips on fiber glass circuit board material. The rings and wires are on opposite sides of the boards, and the boards have been cut and assembled into an interlocking lattice. (b) Transmitted power at 10.5 GHz as a function of refraction angle for both a Teflon sample (blue curve) and a LHM sample (red curve). The two curves were normalized such that the magnitude of both peaks is unity.[Reproduced from [13]]	22
4.1	Dispersion graph for the parallel wave.[Reproduced from [23]]	33
4.2	Dispersion graph for the perpendicular wave. [Reproduced from [23]]	35
4.3	The permittivity (ϵ) as a function of the dimensionless frequency x for the parallel propagation with $x_p = 1.1$	43
4.4	The permeability (μ), n^2 , and n versus x for parallel propagation with $x_m = 0.06$	45
4.5	The permeability (μ), n^2 , and n versus x for parallel propagation with $x_m = 0.08$	46
4.6	The permeability (μ), n^2 , and n versus x for parallel propagation with $x_m = 0.5$	47
4.7	The permittivity (ϵ) as a function of the dimensionless frequency x for the perpendicular propagation with $x_p = 1.1$	48
4.8	The permeability (μ), n^2 , and n versus x for perpendicular propagation with $x_m = 0.06$	49
4.9	The permeability (μ), n^2 , and n versus x for perpendicular propagation with $x_m = 0.08$	50
4.10	The permeability (μ), n^2 , and n versus x for perpendicular propagation with $x_m = 0.1$	51
4.11	(Left) n versus x graph for the parallel wave at $x_m = 0.708$. (Right) n versus x graph for the perpendicular wave at $x_m = 0.1$	52

4.12	The normalized phase velocity $\frac{v_p}{c}$, the normalized group velocity $\frac{v_g}{c}$ and the normalized phase and group velocity combined, respectively, graph for the parallel wave at $x_m = 0.5$	54
4.13	The normalized phase velocity $\frac{v_p}{c}$, the normalized group velocity $\frac{v_g}{c}$ and the normalized phase and group velocity combined, respectively, graph for the perpendicular wave at $x_m = 0.08$	56

Abstract

Since the report made by Veselago in 1968 about materials with negative refractive index, and strictly speaking since the experimental realization in 2000 by R. Shelby, et. al. of artificially constructed materials exhibiting negative index, many investigators and scholars became interested and devote their time and knowledge in search of these negative index (NI) materials, either from artificially engineered materials or to derive them from naturally occurring materials.

This thesis is devoted to the analysis of the electrodynamic and the dispersion properties of magnetized plasma with ferromagnetic grains (MPFG) in a constant magnetic field. A magnetized plasma naturally is not transparent to light for some range of frequency. This range of frequency which the magnetized plasma is not transparent, obviously, is a range in which the permittivity is negative. So, if, in some way, we introduce magnetically active materials into the magnetized plasma in such a way to enhance its magnetic activity we may achieve a magnetic resonance, a dispersion related with magnetic response of magnetized grains to the variable magnetic field. The mathematical analysis and the different graphs against the frequency of the wave show that in a relatively narrow frequency band $\xi\omega_M$ (ω_M is the ferromagnetic resonance frequency) both the magnetic permeability and the electric permittivity have negative value and the MPFG behaves as a NI material. That is, the introduction of the ferrite grains makes the magnetized plasma transparent to the electromagnetic wave for the range of frequency where the ordinary plasma is nontransparent. Moreover, in this range of frequency the phase and group velocity of the electromagnetic wave are opposite, which is one of the criterion for the left-handed media.

Acknowledgements

I would like to express my gratitude to my supervisor Dr Belayneh Mesfin for suggesting me to work on this title, for his guidance and valuable critics and suggestions. I am also indebted to Dr Tilahun Tesfaye for his support and encouragement. I would like to extend my gratitude and appreciation to the Department of Physics, Addis Ababa University, for the unreserved effort to retain the standards and quality of education. I would also like to thank Ministry of Education of Ethiopia and the Educational bureau of Arada region of Addis Ababa for granting me the opportunity to study for my Msc degree.

I also would like to thank my friends Osman Taha and Atalay Bitew for their encouragement, support and to whom I always turn whenever I'm in need of some resources. I want to make a special reference to Leulseged Tefera, Abebe Dissasa, Getachew Mulat and Tilahun Hailu. You have all supported and encouraged me along my journey to my MSc degree and your friendship, confidence in me and company are truly remarkable. To all the current physics graduating students in particular to Getahun Chane, Bellina Dinegdie, Sintayehu, Alemayehu Mossisa, Lakech, Negalign, Taddese, Tedla, and Belay Gemechu. Thanks for your friendship and valuable discussions.

Finally, I want to thank all my family, specially my sisters Abay and Fantu; and my brother Amdie Mengistie for their patience and helpfulness.

Kassu Shiferaw
Addis Ababa, Ethiopia
August 2016

Chapter 1

Introduction

Since the earliest time, mankind had been more familiar with light and its characteristics. Driven by curiosity man had acquired unwavering understanding and control over light and its interaction with materials. The optical property of a medium is represented by a quantity called the index of refraction, n . The index of refraction is the response of a medium to the presence or passage of light. It is also defined as the measure of the “optical density” of a medium.

In every high school and undergraduate physics text books the value of the refractive index of a media is always assumed to be positive. Although there was no hypothesis or experimental base that restrict the values of the refractive index, all known transparent media were described by a refractive index between about 1.2 and 1.9 only at optical frequencies (Excluding semiconductors where it could be as large as 4 in the infrared regions). [1]

In 1968, Viktor G. Veselago [2], a Russian Physicist, suggested the possibility of a media with negative refractive index. In fact, no natural material having negative index of refraction has been, and still is, known. Thus their realization took the path of artificially constructed composite materials and engineered structures that have been called metamaterials.

Veselago concluded that not only should such materials be possible but, if ever

found, would exhibit remarkable properties unlike those of any known materials, giving a twist to virtually all electromagnetic phenomena. [2]

The word “metamaterials” today implies composite materials consisting of structural units much smaller than the wavelength of the incident radiation and displaying properties not usually found in natural materials [1]. Unlike the composite materials which derive their electromagnetic properties from repeated diffraction and multiple scattering, metamaterials entirely depend on resonance for their properties.

Metamaterials (MMs) extend this concept replacing the molecules with manmade structures that might have dimensions of nanometers for visible light or in the case of GHz radiation may be as large as a few millimeters, but still much less than the wavelength. In this way properties are engineered through structure rather than through chemical composition.

This new idea of Veselago did not won the focus and interest of physicists. It was almost about 30 years later, when Pendry, et al. (1996) [3] theoretically suggested and experimentally demonstrated (1999) that a composite medium of periodically arranged thin metallic wires can exhibit a negative permittivity, that the idea gained the interest among the scientific community.

Next, in order to create a medium with negative permeability, Pendry[4] proposed various magnetic resonant structures such as array of cylinders, array of “Swiss Roll” capacitors. In particular, there has been high level of interest in studying materials which can be characterized by simultaneous negative permittivity and permeability over a certain frequency band.

In 2000, Smith, et al. [5] fabricated an NI material using artificially constructed metamaterials (MMs). This negative (refractive) index matterial (NIM) combined a wire structure with $\epsilon < 0$ and a split-ring resonator (SRR) structure with $\mu < 0$ over the same band of frequencies. The fabrication of such a material, a NIM, came as a surprise to many scientists; indeed some believed that n was required by physical laws

to be positive. In fact, it was after an overwhelming theoretical and computational studies and experimental results were presented in favor of negative refraction that the dispute on the matter finally settled [6].

The first demonstration and confirmation of negative refraction was performed in 2001 by Shelby, et al. [7]. Negative refraction was determined by a Snell's Law experiment using a prism shaped MM wedge. A beam of microwave radiation incident on the prism was observed to refract to the opposite side of the surface normal, thus demonstrating negative refraction. For reference, the same beam deflection experiment was performed using a Teflon prism (positive index). The positive index sample deflected the beam to the opposite side of the surface normal at an angle consistent with the known index of the material. These initial results have now been confirmed by numerous researchers, including Parazzoli, et al [8] from Boeing and Houck, et al. from Massachusetts Institute of Technology [6].

With Veselago's negative index material finally a reality, and with numerous experimental confirmations having established the validity of the metamaterials approach, researchers have taken up Veselago's exploration of negative refraction.

Figure 1.1 summarizes some work extending metamaterials response from the initial discovery range - microwave - to both higher and lower frequency ranges; and is arranged from the lowest frequency in the top row to the highest frequencies in the bottom row [6].

Yet another approach to produce NIMs is to use photonic band gap, PBG. PBGs are periodic structures typically constructed from high dielectric materials, that, as their name implies, exhibit frequency range nontransparent to EMW. The dispersion relation describing the propagation modes, also known as Bloch or Floquet modes, are nonlinear and can in some cases lead to negative refraction. Unlike negative index materials in which the group and phase velocities are antiparallel, in PBGs, however, the group velocity and the phase velocity vectors are not parallel. Hence the negative

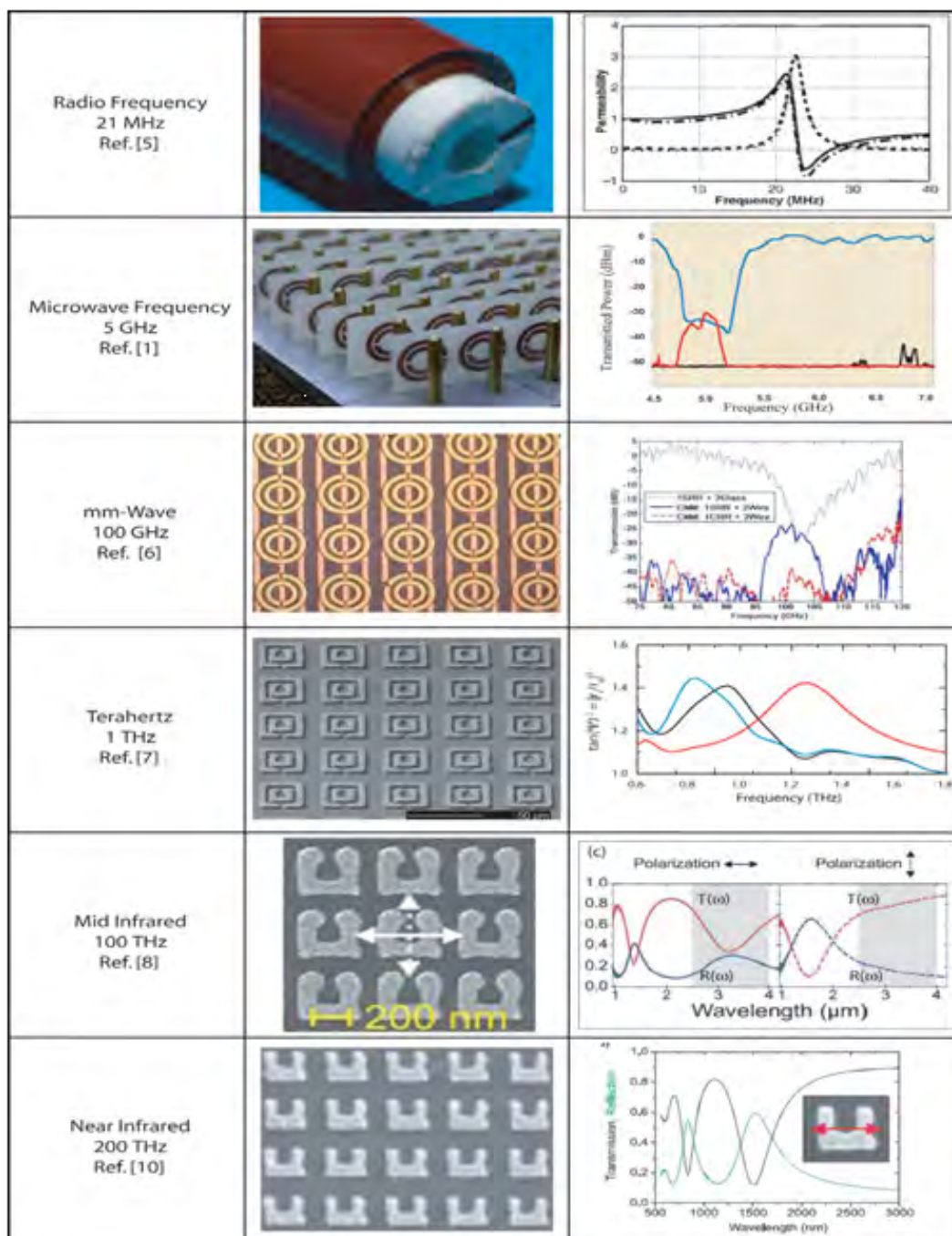


Figure 1.1: Summary of MM results from RF to near optical frequencies. In the left column the frequency ranges in which each MM was demonstrated are depicted. The middle column shows a photo of the MM from each publication, and the third column shows some data detailing the MM response.[Adapted from [6]]

refraction behavior in PBGs is different from NIMs. [9]

Although most negative index materials have been constructed using artificially made metamaterials, scientists currently turning towards using combinations of naturally occurring materials to achieve NIMs.

Recent progresses in the research of electromagnetic metamaterials have been reported by using chiral materials [10], gyrotropic chiral composite materials [11] and it has been demonstrated that a negative index (NI) can be exhibited by magnetodielectric spherical particles, super lattices of natural materials, and uniaxial crystals. There are many theoretical suggestions of various other methods one might use to achieve an NI at near infrared and optical frequencies [6]. Even though the NI in these materials comes about 'naturally', they are still considered as metamaterials since they are engineered in suitable shape and combination.

Chapter 2

Theoretical Background

Practically, the concepts and principles in the study of negative refractive index materials (NIM) are all nothing but that of electrodynamics. The only concept that grant NIMs exceptional status in electrodynamics is the introduction of negative index of refraction.

This chapter presents a brief discussion about the already known electrodynamics concepts and principles vis-a-vis NIMs, how an electromagnetic wave affect and be affected in passing through a NIM and whether there is violation of the laws and equations of physics, in particular optics and electrodynamics, caused by the introduction of negative refractive index. In addition, the last section of this chapter presents the progresses made in the realization of NIMs, the procedures that were and should be carried out in the construction of this materials.

2.1 Basic Concepts and Definitions

2.1.1 Maxwell's Equations and the Constitutive Relations

To understand metamaterials, it is necessary to understand material response to electromagnetic waves (EM) in general. EM response in homogeneous materials is

predominantly governed by two parameters: dielectric permittivity, ϵ , and magnetic permeability, μ .

Let us consider a monochromatic plane wave propagating in an isotropic, homogenous medium. The electric and magnetic components of the plane wave have the form:

$$\vec{E}(\omega, \vec{k}) = \vec{E}_0 e^{i(\vec{k} \cdot \vec{r} - \omega t)} \quad (2.1.1)$$

and

$$\vec{H}(\omega, \vec{k}) = \vec{H}_0 e^{i(\vec{k} \cdot \vec{r} - \omega t)} \quad (2.1.2)$$

respectively, where ω is the angular frequency and \vec{k} is the wave vector. The fundamental macroscopic Maxwell's equations are

$$\nabla \cdot \vec{D} = \rho \quad (2.1.3)$$

$$\nabla \times \vec{E} = -\frac{\partial \vec{B}}{\partial t} \quad (2.1.4)$$

$$\nabla \cdot \vec{B} = 0 \quad (2.1.5)$$

$$\nabla \times \vec{H} = \vec{J} + \frac{\partial \vec{D}}{\partial t}, \quad (2.1.6)$$

where \vec{E} and \vec{H} are the macroscopic electric and magnetic fields, \vec{D} is the displacement field, and \vec{B} is the macroscopic magnetic induction. Similarly, ρ and \vec{J} are the macroscopic net charge and current densities.

The concepts of dielectric permittivity, ϵ , and magnetic permeability, μ , are used to describe the media and their response to electric and magnetic fields, and are called *constitutive parameters*. The constitutive equations are given by

$$\vec{D} = \epsilon \vec{E} = \epsilon_0 \epsilon_r \vec{E} \quad (2.1.7)$$

$$\vec{B} = \mu \vec{H} = \mu_0 \mu_r \vec{H} \quad (2.1.8)$$

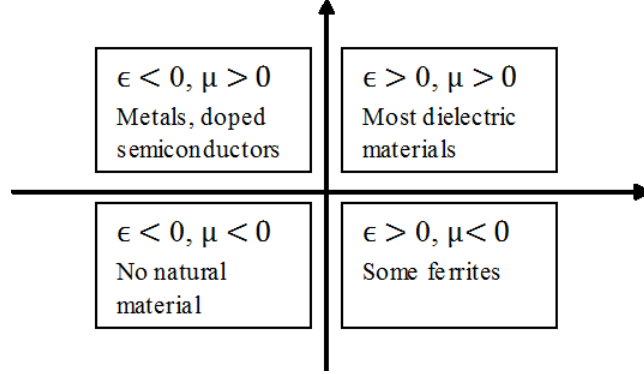


Figure 2.1: Material parameter space characterized by electric permittivity (ϵ) and magnetic permeability (μ).

Substituting these relations in the Maxwell's equations, we obtain

$$\vec{k} \times \vec{E} = \mu\omega\vec{H} \quad (2.1.9)$$

$$\vec{k} \times \vec{H} = -\epsilon\omega\vec{E}. \quad (2.1.10)$$

The dielectric permittivity, ϵ describes the response of a material to the electric component of the electromagnetic wave and the magnetic permeability, μ , to the magnetic component at a frequency ω . The permittivity and the permeability of a medium may be a scalar or a second rank tensor and may be real or complex quantities depending on whether the material is isotropic or not and whether it is dissipative or not. Both of these parameters are typically frequency-dependent complex quantities, and thus there are in total four numbers that completely describe the response of an isotropic material to EM radiation at a given frequency. That is,

$$\epsilon(\omega) = \epsilon_1(\omega) + i\epsilon_2(\omega) \quad (2.1.11)$$

$$\mu(\omega) = \mu_1(\omega) + i\mu_2(\omega). \quad (2.1.12)$$

Depending on the value of their permittivity and permeability, materials can be categorized into four groups, as shown in Fig. 2.1.

2.1.2 Phase Velocity, Group Velocity and Poynting Vector

The concept of negative index of refraction itself seemed to be new and unusual, although it had been introduced already in 1968 by the general consideration of the electrodynamics properties of the materials with simultaneously negative values of the dielectric permittivity ϵ and magnetic permeability μ .

The choice of a negative sign for both ϵ and μ does not cause mathematical contradictions; in particular this does not change the classical expression for n . The optical and electromagnetic phenomena are related by the simple equation, known also as Maxwell's relation:

$$n = \pm\sqrt{\epsilon_r\mu_r} \quad (2.1.13)$$

where n is called the index of refraction of the medium and it describes the speed of the electromagnetic wave in the medium. That is,

$$v = \frac{c}{n}, \quad (2.1.14)$$

where c the speed of the electromagnetic wave in free space and v is the speed of the electromagnetic wave in the medium. When both ϵ and μ are positive n will be positive, and if both ϵ and μ are negative n will be negative, otherwise n is a complex number.

For a monochromatic plane wave, such that $\vec{E} = \vec{E}_0 \cos(kz - \omega t)$ propagating in the \hat{z} direction, considering a constant phase yields

$$\frac{d}{dt}(kz - \omega t) = 0 \quad (2.1.15)$$

$$v_p = \frac{dz}{dt} = \frac{\omega}{k}, \quad (2.1.16)$$

where v_p is called the phase velocity. In free space $v_p = c$. In the case of a more general lossless non-dispersive medium the phase velocity is the velocity of light in the medium and it is usually less than the speed of light in free space.

On the other hand, in a dispersive media where the phase velocity is dependent on the frequency of the electromagnetic wave, the phase velocity can be typically larger than the speed of light in the medium. This does not violate the principle of special relativity since the phase velocity is not associated with a transport of energy, or more strictly, transmission of a signal.

In reality, all physical signals are composed of frequencies that spread over a certain frequency band and the signal is thus a slowly varying envelope containing a rapidly oscillating wave. Therefore, in general the group velocity is given by

$$v_g = \frac{d\omega}{dk}. \quad (2.1.17)$$

The group velocity is considered as the velocity of the envelope or the packet, and corresponds to the velocity of propagation of the energy in many cases. Expressing the group velocity in terms of the phase velocity, we get

$$\frac{1}{v_g} = \frac{1}{v_p} + \omega \frac{d}{d\omega} \frac{1}{v_p}. \quad (2.1.18)$$

From (2.1.18), we may have three cases. These are

1. Non-dispersive case: If the second term in the right side of (2.1.18) is zero, that is, if there is no frequency dispersion,

$$\frac{\partial}{\partial \omega} \left(\frac{1}{v_p} \right) = 0, \quad v_g = v_p.$$

2. Normal dispersion,

$$\frac{\partial}{\partial \omega} \left(\frac{1}{v_p} \right) > 0, \quad v_g < v_p.$$

Since v_p can be larger than the velocity of light inside the medium, it can easily be shown that v_g is in fact lower than this limit.

3. Anomalous dispersion

$$\frac{\partial}{\partial \omega} \left(\frac{1}{v_p} \right) < 0, \quad v_g > v_p.$$

In this case, however, the group velocity loses its meaning as signal velocity, which has to be defined in terms of the electromagnetic energy flow.

Generally, the group velocity is given by the vectorial equation

$$\vec{v}_g = \nabla_{\vec{k}} \omega. \quad (2.1.19)$$

This gradient relationship indicates that the direction of the group velocity is normal to the iso-frequency contour in the spectral domain.

From Maxwell's equation, Eq.(2.1.4 and 2.1.5), with time dependency $e^{-i\omega t}$, we get

$$\vec{k} \times \vec{E} = \mu \omega \vec{H} \quad (2.1.20)$$

$$\vec{k} \times \vec{H} = -\epsilon \omega \vec{E}. \quad (2.1.21)$$

From these equations it is clear that the triad \vec{k} , \vec{E} , and \vec{H} form a right-handed triplet if $\epsilon > 0$ and $\mu > 0$ but if $\epsilon < 0$ and $\mu < 0$ simultaneously \vec{k} , \vec{E} , and \vec{H} form a left-handed triplet. Because of this negative index materials are also called Left-Handed Materials, LHM.

The Poynting vector, \vec{S} , which represents the energy flux, is given by

$$\begin{aligned} \vec{S} &= \vec{E} \times \vec{H} \\ &= \vec{E} \times \left[\frac{1}{\omega \mu} (\vec{k} \times \vec{E}) \right]. \end{aligned} \quad (2.1.22)$$

Assuming $\vec{E} = \hat{e} E_0$, where \hat{e} the polarization direction, we get

$$\vec{S} = \frac{1}{\omega \mu} [k(\hat{e} \cdot \hat{e}) - (\vec{k} \cdot \hat{e})\hat{e}] E_0^2. \quad (2.1.23)$$

But $\vec{k} \cdot \hat{e} = 0$, and hence

$$\vec{S} = \frac{\vec{k}}{\omega \mu} E_0^2, \quad (2.1.24)$$

which shows that the Poynting vector, \vec{S} , is directed in opposite direction to the wave vector, \vec{k} .

This implies that the Poynting vector, \vec{S} , together with \vec{E} and \vec{H} always form right-handed triplet, regardless of what the simultaneous sign of ϵ and μ . Thus, in a media in which ϵ and μ are simultaneously negative, the Poynting vector \vec{S} , and the wave vector \vec{k} , are antiparallel. The direction of the energy flow coincides with the group velocity, whereas the phase velocity is in the direction of the wave vector, \vec{k} . This implies that when ϵ and μ are simultaneously negative the phase velocity and the group velocity are antiparallel.

2.2 Laws of Physics in NIMs

The other logical question that comes into mind is that whether the laws and equations of physics, specifically, the laws and equations of electrodynamics and optics, are valid or not in a media in which ϵ and μ are simultaneously negative. How does an electromagnetic wave affect and affected by a media having ϵ and μ simultaneously negative?

To answer this question one needs to consider all the laws and equations of electrodynamics and optics that involve the constitutive parameters n , ϵ and μ . Most of the laws and equations of electrodynamics and optics are formulated for nonmagnetic materials where the magnetic permeability $\mu = 1$. In some cases the replacement of the permeability by $\mu \neq 1$ may lead to an incorrect equation.

In their review paper, Veselago, et al. [12], categorized the laws and equations of electrodynamics and optics into three groups: those equations, such as Snell's law, Cherenkov Effect and Doppler Effect, which may be corrected by changing $n = \sqrt{\epsilon}$ to $n = \sqrt{\epsilon\mu}$ and taking negative n ; those equations, such as Fresnel's formula, which may be corrected by changing $n = \sqrt{\epsilon}$ not to $n = \sqrt{\epsilon\mu}$ but to $\sqrt{\epsilon/\mu} = 1/Z$, where

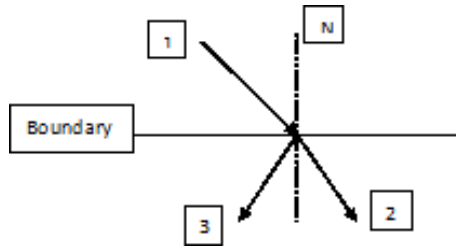


Figure 2.2: Snell's law for positive ϵ and μ (path 1-2) and for negative ϵ and μ (path 1-3).

Z is the impedance of the wave and which is positive; and the third group are those, such as the Brewster angle, which require a complete change of equation.

The phenomena associated with electromagnetic wave propagating in materials with ϵ and μ simultaneously negative is almost reversed compared with the positive materials. For example, in Snell's refraction, the refracted ray will be in the same side of the normal as the incident ray Fig. 2.2, the Doppler shift is reversed, with a light source moving toward an observer resulting in a reduced frequency and the Cherenkov radiation from a charge passing through the material is emitted in the opposite direction to the charge's motion rather than in the forward direction.

The origin of this newly predicted behavior can be traced to the distinction between the group velocity, which characterizes the flow of energy, and the phase velocity, which characterizes the movement of the wave fronts. In conventional materials, the group and phase velocities are parallel. By contrast, the group and phase velocities point in opposite directions when $\epsilon < 0$ and $\mu < 0$. The reversal of phase and group velocity in a material implies a simply stated but very serious consequence: The sign of the refractive index, n , must be taken as negative.

2.3 Metamaterials

Despite the fact that no material having negative ϵ and μ within the same frequency band found naturally, there is no any physical reason that prohibits their existence. Since the index of refraction of such materials is a real number, negative index materials are transparent to light [13].

It is expected that these left-handed materials may exhibit properties that are different and may even show properties that were not observed before in natural media. Because finding such materials naturally is difficult, their realization took the route through the artificially made materials. All the negative index materials that have been developed today are obtained by merging together two artificially structured materials that show separately a negative dielectric permittivity and negative magnetic permeability within the same frequency range. The two structures that separately show $\epsilon < 0$ and $\mu < 0$ and that are going to be put together, each should function independently without strongly interfering with each other, a condition that is not always automatically satisfied.

This section discusses the different possible ways that has been used in constructing the negative dielectric materials, the negative magnetic materials and the composite that behaves as a negative index material formed by combining the two.

2.3.1 Materials with Negative Permittivity

It is a known fact that naturally occurring materials, such as plasma of negative charges and some precious metals, like silver and gold, yield a negative response to the electric component of light. Any metal below its plasma frequency (the frequency at which it becomes transparent) yields negative values of the permittivity. This negative permittivity response results from the fact that the free electrons in the metal screens external electromagnetic radiation.

Alternatively, it is also possible to apply circuit models which behave as resistors, capacitors, or inductors that exhibits negative electric response. Many decades ago researchers fabricated structures having $\epsilon < 0$ using arrays of conducting wires and other unique shapes. This technology was recently reintroduced with a more physics-oriented understanding. Currently, variations of the wire lattice being used to create negative permittivity media include straight wires, cut-wire segments, and loop wires.

Starting from Lorentz force, neglecting the contribution of the magnetic field, we can obtain a general expression for the dielectric constant or the relative permittivity as

$$\epsilon_r(\omega) = 1 + \frac{\omega_p^2}{\omega_0^2 - \omega(\omega + i\gamma)} = 1 - \frac{\omega_p^2}{\omega^2 - \omega_0^2 + i\gamma\omega}, \quad (2.3.1)$$

where ω_0 is the resonant or the harmonic binding frequency, γ is the damping constant, ω is the angular frequency of the electromagnetic wave and the plasma frequency, $\omega_p^2 = Ne^2/m\epsilon_0$. From this equation one can see that for small dissipation the permittivity will be negative over the range frequency $\omega_0 < \omega < \omega_p$.

The plasma frequencies for many metals, such as gold and silver, alkali metals such as lithium, sodium and potassium, and others such as aluminum, lie in the ultraviolet region of the spectrum. Under the free electron approximation, ω_0 is taken as zero. This means that the permittivity of metals is always negative below the plasma frequency. That is, setting $\omega_0 = 0$, Eq. (2.3.1) reduces to

$$\epsilon_r(\omega) = 1 - \frac{Ne^2/m\epsilon}{\omega(\omega + i\gamma)} = 1 - \frac{\omega_p^2}{\omega(\omega + i\gamma)}. \quad (2.3.2)$$

From the equation it is clear that for negligible dissipation, the real part of the permittivity is negative when $\omega < \omega_p$.

Some dielectric materials can also have interesting spectral bands with $\epsilon < 0$. Because the dissipation in dielectric materials is much lesser than that in metals, such dielectric materials have great potential in the design of metamaterials for use as negative dielectric materials, specially, at low frequencies (near-mid infrared and

lower frequencies). The disadvantage of these dielectric materials is that the frequency range over which $\epsilon < 0$ is often narrow unlike in metals.

It is obvious from the generic equation of the permittivity that as the dissipation becomes large, the dielectric permittivity becomes more of a complex number and, in addition, at low frequencies the dielectric permittivity would have a very large magnitude implying that all radiation would decay within very short distances in the medium.

Because of these shortcomings of the naturally occurring materials scientists turn their focus towards constructing composite materials. Pendry, et al. [3, 4] proposed that dilute arrays of thin metallic wires would have very low plasma frequency. It is simply an array of periodically placed infinitely long straight parallel very thin conducting wires and the electric field will be applied parallel to the wires, Fig. 2.3. This structure will behave as anisotropic medium. By placing the wires orthogonally to each other in 3D it can be made isotropic. The dielectric permittivity of this proposed metallic thin wire mesh structure obeys the Drude-Lorentz model, Eq. (2.3.2),

$$\epsilon_r(\omega) = 1 - \frac{\omega_p^2}{\omega(\omega + i\gamma)},$$

where the effective plasma frequency is [1], *penHolYg96*

$$\omega_p^2 = \frac{2\pi c^2}{a^2 \ln(a/r)}, \quad (2.3.3)$$

and the effective damping constant is [1]

$$\gamma = \frac{\epsilon_0 a^2 \omega_p^2}{\pi r^2 \sigma}, \quad (2.3.4)$$

where r is the radius of the wires which are placed periodically at a distance a in a square lattice with $a \gg r$ and c is the speed of light.

Another variety of the wire mesh is the cut wire in which instead of the infinitely long straight wires, discontinuous segments of wires are used. In this structure the

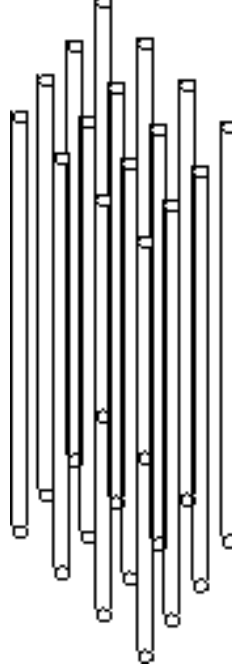


Figure 2.3: An array of nonmagnetic, infinitely long, thin metal wires behaves as a low frequency plasma for an electric field oriented along the wires.

gap between the wires acts as a capacitor which coupled with the inductor inherent in the straight wires acts as an LC circuit which introduces a resonant frequency in the equation of the effective permittivity. Consequently, the effective permittivity for this composite is given [1]

$$\epsilon_r(\omega) = 1 - \frac{\omega_p^2}{\omega^2 - \omega_0^2 + i\gamma\omega}, \quad (2.3.5)$$

where the resonant frequency is [1]

$$\omega_0 = \frac{2\pi c^2 d}{\epsilon_m A(\ell + d) \ln(a/r)}, \quad (2.3.6)$$

where ϵ_m is the relative permittivity of the medium inserted, d the separation distance between the segments, A is the area of the segment cross section and ℓ the length of the segments.

In such metamaterials since the effective density, the effective mass and the plasma frequency can be tuned by geometry, they are much greater flexible than conventional materials and hence the region of moderately negative values can be made to occur at nearly any frequency range, from low radio frequency to the optical.

2.3.2 Materials with Negative Permeability

Although there are naturally occurring materials with electric response almost at any frequency and even with negative electric permittivity, typically in the optical, for metals, or at least in the THz to infrared region for semiconductors and insulators [1], surprisingly, there are no naturally occurring materials with magnetic response beyond the microwave frequencies. Unlike the electric response, at high frequencies, beyond the gigahertz region, even the magnetic response of naturally existing materials tends to vanishes, let alone exhibiting negative magnetic permeability.

Magnetization actually arises from unpaired electronic spins or electronic orbital currents. However, both these effects respond to electromagnetic waves only at low frequencies, which is the fundamental reason why there are no magnetic materials at high frequencies [14]. Particularly, there is no a single substance known which could be isotropic and have $\mu < 0$. The nonexistence of such materials is ascribed to the fact that the nonexistence of magnetic charges or magnetic monopoles, but dipoles [2].

Consequently, the only alternative to have negative permeability is through structured materials. In this section we discuss about structured materials which give rise to magnetic response and, in particular, to a negative magnetic permeability.

A magnetic response can be obtained if currents can be induced to circulate in closed loops. Moreover, introducing a resonance into the element should enable a very strong magnetic response, potentially one that can lead to a negative permeability.

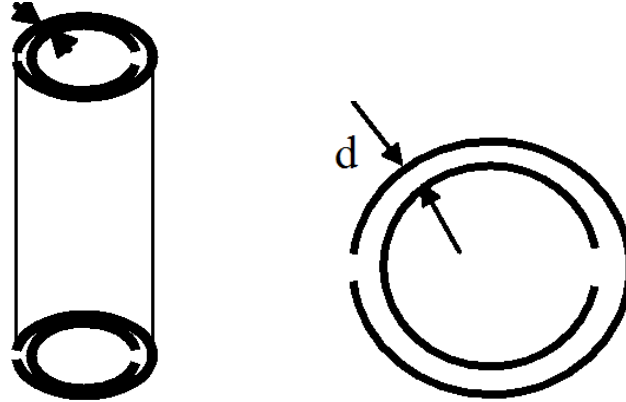


Figure 2.4: (Left) Split ring resonator. (Right) Split ring in flat two dimension. d is the separation between the rings.

In 1999, Pendry, et al. [4] proposed a variety of structures that, they predicted, would form magnetic metamaterials. These nonmagnetic structures consisted of arrays of wire loops or tubes, Fig. 2.4, in which an external applied magnetic field along the tubes could induce a circumferential surface current, thus producing an effective magnetic response.

By introducing a gap, which acts as capacitive element in each wire loops, a rich resonant response can be induced. Such structures, that is, wire loops with capacitive gaps have become well known and named *split-ring resonators*, SRR.

Today the split-ring resonator has become the basis of most of the metamaterials exhibiting negative magnetic permeability. The SRR consists of a planar set of concentric incomplete rings, each ring with gaps, somewhat forming semicircles, as shown in Fig. 2.4. Essentially, the SRR works on the principle that the magnetic field of the electromagnetic radiation drives a resonant LC circuit, which results in a dispersive effective magnetic permeability.

Another variety of resonant unit proposed by Pendry, et al. is the Swiss Roll. The Swiss Roll is simply a sheet of metal rolled in the form of cylinder and with each roll

being separated by an insulator. The generic equation of the effective permeability of these structures is [15]

$$\mu_{eff}(\omega) = 1 - \frac{F\omega_0^2}{\omega^2 - \omega_0^2 - i\gamma\omega}. \quad (2.3.7)$$

where F the filling fraction is

$$F = \frac{\pi r^2}{a^2}$$

Recently, an SRR composite designed to exhibit a magnetic resonance at THz frequencies was fabricated [13]. Scattering experiments confirmed that the SRR medium had a magnetic resonance that could be tuned throughout the THz band by slight changes to the geometrical SRR parameters.

2.4 Materials with negative refractive index

In the previous sections, it was mentioned that the possible alternative to realize negative index metamaterial is by combining a negative permittivity and a negative permeability elements. It should be noted, of course, that putting a material with $\mu < 0$, such as an SRR, into a material having $\epsilon < 0$, such as a metal, would not result in a negative refractive index material. This is because the metal will, somewhat, shield the SRR unit such that the electromagnetic radiation may not be sufficient to invoke magnetic resonance. Generally, to produce a negative index metamaterial by putting together a $\epsilon < 0$ and $\mu < 0$ materials, it is essential that the radiation to the units is sufficient enough to excite the electric and magnetic resonance, there should be a frequency range in which the frequency range of the $\epsilon < 0$ and $\mu < 0$ material coincide, and there should not be interference between the electric and magnetic resonance.

There are demonstrations and experimental verifications supporting that by applying this method a composite medium with negative index could be realized. In

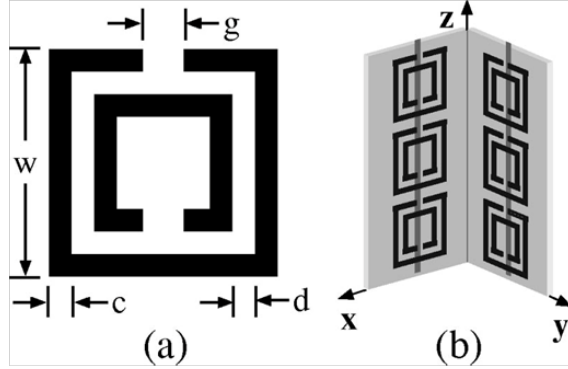


Figure 2.5: (a) Diagram of a single split-ring resonator (SRR), $c = 50.25 \text{ mm}$, $d = 50.30 \text{ mm}$, $g = 50.46 \text{ mm}$, $w = 52.62 \text{ mm}$, and the SRR is square. (b) Each unit cell has six copper SRRs and two wire strips on thin fiberglass boards. The wire strips are 1 cm long, centered on the SRRs, and on the opposite side of the board from the SRRs. The angle between the fiberglass boards is 90° to make square unit cells with a lattice constant of 5.0 mm . [Extracted from [16]]

2000, Smith, et al. [5] was the first to introduce a composite structure by combining SRRs with thin wire and showed to have a frequency band over which ϵ and μ were both negative. The negative μ occurred at frequencies above the resonant frequency of the SRR structure and the wire structure exhibits negative ϵ below a cutoff frequency. Then the composite was made to have an overlapping region of frequency where both $\epsilon < 0$ and $\mu < 0$.

After Smith et al. demonstration, which was performed on one dimensional left-handed material composed of array of unit cells each consist of a SRR and a straight conducting wire, Shelby, et al., in 2001 [7] presented an experiment on two dimensionally isotropic left handed structure formed by placing two SRR orthogonally with wire strips mounted behind the SRR.

Shelby, et al. achieved 2D isotropy by placing the SRR along two orthogonal axes. In this transmission experiment, because the wires are very thin compared with those used in Smith, et al. transmission experiment, two thin wires per each cell were used

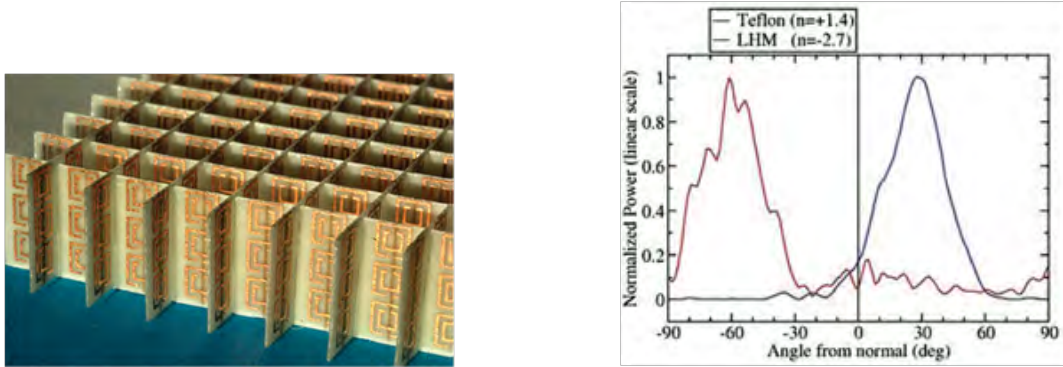


Figure 2.6: (a) The LHM sample consists of square copper split ring resonators and copper wire strips on fiber glass circuit board material. The rings and wires are on opposite sides of the boards, and the boards have been cut and assembled into an interlocking lattice. (b) Transmitted power at 10.5 GHz as a function of refraction angle for both a Teflon sample (blue curve) and a LHM sample (red curve). The two curves were normalized such that the magnitude of both peaks is unity.[Reproduced from [13]]

to compensate for the density. Then the SRR and the wire strips lithographically printed on a circuit board, Fig. 2.6.

Following these experiments, two more experiments on Snell's law of refraction were reported. The experiments presented were performed on a left-handed media fabricated from a periodic array of copper SRR and wires which then made into prism shape. The experiment was done on the left-handed material as well as on a similarly shaped Teflon sample as a control.

In 2001, Shelby, et al. displayed Snell's law experiment in which a beam of microwave radiation incident on the prism was observed to refract to the same side of the surface normal as the incident beam, while the same beam incident on a Teflon prism (positive index) deflected to the opposite side of the surface normal at an angle consistent with the known index of the material. These initial results have now been confirmed by numerous researchers, including Parazzoli, et al. [8].

These experiments, which have been demonstrated at microwave frequencies, encouraged researchers to extend the range of frequency of metamaterials to the terahertz, infrared, and visible bands. Progress in metamaterials has been rapid. The scaling of artificial structures has already been demonstrated from radio frequencies to millimeter-wave, far infrared, mid-infrared, and near infrared wavelengths, spanning nearly seven orders of magnitude in frequency.

Chapter 3

Contemporary Ideas and New Frontiers in Search of Metamaterials

Veselago in his paper suggested the possibility of negative materials from naturally occurring anisotropic substances [2]. He pointed out that the permittivity and permeability of such materials are tensors. Among these substances are gyrotropic substances such as plasma contained in magnetic substances, ferromagnets, antiferromagnets, chiral substances, and plasma with magnetic grains embedded in it. Many scientists have been involved in studying various potential metamaterials and there have been many theoretical as well as experimental analysis supporting these naturally occurring anisotropic materials as a potential negative refractive index materials.

This chapter discusses about the basic equations and the propagation of electromagnetic wave in chiral material, anisotropic, and bianisotropic materials. Material media, in Maxwell's theory of electromagnetism, are described by the constitutive parameters. Generally speaking, a medium can be characterized as homogeneous, inhomogeneous, isotropic, anisotropic, bianisotropic, depending on the particular form of the constitutive relations.

3.1 Chiral Materials

The term chiral is used to describe a material that is non-superimposable on its mirror image. The literal origin of chiral is from the Greek word for hand [14]. Some crystals have the ability to rotate the plane of a linearly polarized plane light wave passing through them, a property known as optical activity or rotary power. Optical activity is caused by chirality, either of the molecules making up the substance, or in the helical arrangement of the atomic or molecular constituents in a crystal.

Arago (1811) was the first who saw the manifestation of optical activity in a quartz crystal. He observed that the quartz crystal rotates the plane of polarization of a linearly polarized light which passes along the crystal optic axis. Following Argos observation, Biot (1812) proved that the dependency of the optical activity on the thickness of the crystal plate and on the wavelength of the light and Fresnel (1821), showed that a linearly polarized light ray of a crystal quartz separates into two circularly polarized rays of light - so called right and left handed - having different phase velocities. Pasteur (1840's) postulated that molecules are three dimensional objects and that the optical activity of a medium is caused by the chirality of its molecules. [17]

In 2004, Pendry [17] discussed the possibility to achieve negative refraction in chiral metamaterials and showed that they are simpler than the regular metamaterials, which require both electric and magnetic resonances to have negative values. In chiral metamaterials neither ϵ nor μ needs to be negative. Pendry then proposed a practical model of a chiral metamaterial working in the microwave regime with twisted Swiss rolls as elemental structures.

Despite all these, the chirality of natural media usually is not very strong and the corresponding optical activity is weak. Chiral metamaterials, however, constructed either from intrinsically chiral materials or derive their chiral properties from the

chiral geometric structure of the metamaterial units, can be made to strongly and resonantly enhance the chiral properties via chiral scatterers [1, 17].

Unlike conventional negative index material designs, such as the split-ring resonator type design, the chiral negative index material does not require simultaneously negative permittivity and permeability, and, therefore, the chiral design can offer much simpler geometry and a more efficient way to realize negative refraction index. Obviously chiral materials offer a relatively simpler route to negative refraction and hence, this subject has been constantly approached by researchers [1].

Because they offer a simpler route to negative refraction, nowadays, chiral metamaterials are one of the most interesting subjects that are being studied [10, 14, 18]. The chiral metamaterials with large optical activity have also been proposed and made for polarization control applications at microwave and optical frequencies. Researchers have been studying chiral metamaterial design with strong tunable optical activity in a relatively wide frequency bands with low transmission losses, makes it a very efficient material for tunable polarization [17].

Chiral media are categorized under bi-isotropic medium and the constitutive relation of chiral media is the same as reciprocal bi-isotropic media, which is given by [17]

$$\vec{D} = \epsilon\epsilon_0\vec{E} - i\kappa\sqrt{\epsilon_0\mu_0}\vec{H}, \quad (3.1.1)$$

$$\vec{B} = \mu\mu_0\vec{H} + i\kappa\sqrt{\epsilon_0\mu_0}\vec{E}, \quad (3.1.2)$$

where κ is the chiral parameter.

Substituting (3.1.1) in Maxwell's equations, with time dependency $e^{-i\omega t}$ yields

$$\nabla \times \vec{E} = i\omega\vec{B} = i\omega\mu\mu_0\vec{H} - \omega\kappa\sqrt{\epsilon_0\mu_0}\vec{E}, \quad (3.1.3)$$

$$\nabla \times \vec{H} = -i\omega\vec{D} = -i\omega\epsilon\epsilon_0\vec{E} - \omega\kappa\sqrt{\epsilon_0\mu_0}\vec{H}. \quad (3.1.4)$$

Manipulating the above equations, it can be shown that the refractive index for

chiral media takes the form [1, 17, 19, 20]:

$$n_{\pm} = \sqrt{\epsilon\mu} \pm \kappa, \quad (3.1.5)$$

where “+” and “−” refer, respectively, to the right-handed and left-handed circularly polarized eigenstates and κ is the chirality parameter. This implies that in principle strong enough chirality is sufficient to achieve negative refraction for one circular polarization. At microwave frequencies, the chiral medium can be realized artificially using miniature wire spirals or conducting springs.

3.2 Anisotropic and Bianisotropic Media

The propagation of electromagnetic waves in anisotropic and bianisotropic media is a topic that has been studied for many years, originally because these types of media can be directly found in nature and later because they were realized in the laboratory. Anisotropic medium is a medium in which the electrical and/or magnetic properties of a medium depend upon the directions of field vectors. The relationships between fields can be written in the form:

$$\vec{D} = \epsilon_0 \bar{\epsilon} \cdot \vec{E}, \quad (3.2.1)$$

$$\vec{B} = \mu_0 \bar{\mu} \cdot \vec{H}, \quad (3.2.2)$$

where $\bar{\epsilon}$ and $\bar{\mu}$ are the relative permittivity and permeability tensors, respectively. Anisotropic materials may be divided into two classes. One of these classes of anisotropic materials is those in which the natural modes of propagation are linearly polarized, and for such materials the permittivity and permeability components are symmetric; that is, $\epsilon_{ij} = \epsilon_{ji}$ and $\mu_{ij} = \mu_{ji}$. The other class is those in which the natural modes of propagation are circularly polarized waves, called gyrotropic media, and the permittivity or permeability components for lossless media are antisymmetric, having $\epsilon_{ij} = -\epsilon_{ji}$ and $\mu_{ij} = -\mu_{ji}$.

In the Maxwell's equation, with time dependency $e^{-i\omega t}$, substituting the constitutive relations (3.2.1) gives

$$\nabla \times \vec{E} = i\omega\mu_0\bar{\mu} \cdot \vec{H}, \quad (3.2.3)$$

$$\nabla \times \vec{H} = -i\omega\epsilon_0\bar{\epsilon} \cdot \vec{H}. \quad (3.2.4)$$

Solving (3.2.3) for \vec{H} and substituting in (3.2.4) yields the dispersion relation as

$$\bar{\mu}^{-1} \cdot (\vec{k} \times \bar{I})^2 + \omega^2\mu_0\epsilon_0\bar{\epsilon} = 0, \quad (3.2.5)$$

where \bar{I} is a unit dyadic tensor. Using $\bar{k} = \vec{k} \times \bar{I}$, we get

$$\bar{\mu}^{-1} \cdot \bar{k}^2 + \omega^2\mu_0\epsilon_0\bar{\epsilon} = 0. \quad (3.2.6)$$

On the other hand, bianisotropic media are a special type of materials whose properties are characterized by the magnetoelectric as well as the permittivity and permeability tensors. Due to strong magnetoelectric couplings, the wave propagation in bianisotropic media is usually described by high order dispersion relations with circularly or elliptically polarized waves. Because of these features, bianisotropic plays important role in the pursuit of negative permeability and left-handed metamaterials.

The constitutive relations of a bianisotropic medium relate \vec{D} and \vec{B} to both \vec{E} and \vec{H} . The constitutive relation in the Telegen model is [1]

$$\vec{D} = \bar{\epsilon} \cdot \vec{E} + \bar{\xi} \cdot \vec{H}, \quad (3.2.7)$$

$$\vec{B} = \bar{\mu} \cdot \vec{H} + \bar{\zeta} \cdot \vec{E}, \quad (3.2.8)$$

where $\bar{\epsilon}$, $\bar{\mu}$, $\bar{\xi}$ (xi), and $\bar{\zeta}$ (zeta) are in general arbitrary tensors representing the properties of the medium and are related to the relative quantities $\bar{\epsilon}$, $\bar{\mu}$, $\bar{\xi}$, and $\bar{\zeta}$ by

$$\bar{\epsilon} = \epsilon_0\bar{\epsilon}, \quad \bar{\mu} = \mu_0\bar{\mu}, \quad \bar{\xi} = \xi_0\bar{\xi}, \quad \bar{\zeta} = \zeta_0\bar{\zeta}. \quad (3.2.9)$$

In general, the tensors $\bar{\epsilon}$ and $\bar{\mu}$ have the form:

$$\bar{\epsilon} = \epsilon_0 \begin{pmatrix} \epsilon_{11} & \epsilon_{12} & \epsilon_{13} \\ \epsilon_{21} & \epsilon_{22} & \epsilon_{23} \\ \epsilon_{31} & \epsilon_{32} & \epsilon_{33} \end{pmatrix}, \quad \bar{\mu} = \mu_0 \begin{pmatrix} \mu_{11} & \mu_{12} & \mu_{13} \\ \mu_{21} & \mu_{22} & \mu_{23} \\ \mu_{31} & \mu_{32} & \mu_{33} \end{pmatrix}. \quad (3.2.10)$$

Chapter 4

Magnetized Plasma with Ferromagnetic Grains

Among the promising naturally occurring materials, from which NIMs may be constructed, is the magnetized plasma. Recently there have been intensive studies of magnetized plasmas with embedded ferromagnetic grains[21, 22]. This chapter, in the first section, discusses about the electrodynamics of the magnetized plasma, the dispersion relation and electric permittivity tensor. The second section deals with the main subject of this thesis. It presents a detailed analysis of electromagnetic waves in MPFG, the dispersion relation, the permittivity and the permeability tensors.

4.1 Electromagnetic Waves in Magnetized Plasma

Magnetized plasma has been recently investigated to show interesting electromagnetic properties such as magnetic field induced transparency[23, 24]. In this section we present a brief review of high frequency waves in cold magnetized plasma, where ions motion and collision is ignored.

Assuming an external magnetic field $\vec{B} = B\hat{z}$ and a plane wave, the relevant

Maxwell's equations are:

$$\nabla \times \vec{E} = i\omega\vec{B}, \quad (4.1.1)$$

$$\nabla \times \vec{B} = \mu_0(j - i\omega\epsilon_0\vec{E}),$$

$$\nabla \times \vec{B} = -i\omega\epsilon_0\mu_0\left(\vec{I} + i\frac{\vec{\sigma}}{\omega\epsilon_0}\right)\vec{E},$$

$$\nabla \times \vec{B} = -i\omega\mu_0\bar{\epsilon}\vec{E}. \quad (4.1.2)$$

Substituting (4.1.2) in (4.1.1) yields, with

$$\bar{\epsilon} = \frac{\bar{\bar{\epsilon}}}{\epsilon_0}$$

, we get

$$\vec{k} \times \vec{k} \times \vec{E} + \frac{\omega^2}{c^2}\bar{\epsilon}\vec{E} = 0. \quad (4.1.3)$$

The relative permittivity tensor $\bar{\epsilon}$ is given by [24]

$$\bar{\epsilon} = \begin{pmatrix} \epsilon_1 & -i\epsilon_2 & 0 \\ i\epsilon_2 & \epsilon_1 & 0 \\ 0 & 0 & \epsilon_3 \end{pmatrix}, \quad (4.1.4)$$

where

$$\epsilon_1 = 1 - \frac{\omega_p^2}{\omega^2 - \omega_c^2}, \quad (4.1.5)$$

$$\epsilon_2 = \pm \frac{\omega_c\omega_p^2}{\omega(\omega^2 - \omega_c^2)}, \quad (4.1.6)$$

$$\epsilon_3 = 1 - \frac{\omega_p^2}{\omega^2}, \quad (4.1.7)$$

where the plus is for the proton and the minus sign for the electron. Taking the direction of the electromagnetic wave to be in the xz -plane, i.e., $\vec{k} = k\hat{x} + k\hat{z}$, Eq. (4.1.3) in matrix form will become

$$\begin{pmatrix} \epsilon_1 - n_z^2 & -i\epsilon_2 & n_x n_z \\ i\epsilon_2 & \epsilon_1 - (n_x^2 + n_z^2) & 0 \\ n_z n_x & 0 & \epsilon_3 - n_x^2 \end{pmatrix} \begin{pmatrix} E_x \\ E_y \\ E_z \end{pmatrix} = 0 \quad (4.1.8)$$

There are two main alternative directions of the wave relative to the applied magnetic field direction: perpendicular and parallel to the direction of the magnetic field.

4.1.1 Electromagnetic wave parallel to B

If the direction of the wave is along \vec{B} , that is, $\vec{k} = k\vec{z}$ then in Eq. (4.1.8) setting $n_x = 0$, $n_z = n$ and considering transverse electric component gives

$$(\epsilon_1 - n^2)E_x - i\epsilon_2 E_y = 0, \quad \text{or} \quad \frac{iE_x}{E_y} = \frac{\epsilon_2}{n^2 - \epsilon_1} \quad (4.1.9)$$

$$i\epsilon_2 E_x + (\epsilon_1 - n^2)E_y = 0 \quad \text{or} \quad \frac{iE_x}{E_y} = \frac{n^2 - \epsilon_1}{\epsilon_2}. \quad (4.1.10)$$

Equating (4.1.9) and (4.1.10) and solving for n , we obtain

$$n^2 = \epsilon_1 \pm \epsilon_2, \quad (4.1.11)$$

and the dispersion relation is

$$n^2 = 1 - \frac{\omega_p^2}{\omega(\omega \pm \omega_c)}. \quad (4.1.12)$$

The minus sign is called R-wave, *right circularly polarized* wave and the plus sign is called L- wave, *left circularly polarized* wave.

There are two properties called *cutoff* and *resonance* frequencies. Cutoff is any frequency ω at which the wave number $k \rightarrow 0$. Resonance is any frequency ω at which the wave number $k \rightarrow \infty$. The cutoff frequencies for the left and right waves are then given by

$$\omega_{R/L} = \pm \frac{\omega_c}{2} + \sqrt{\omega_p^2 + \frac{\omega_c^2}{4}} \quad (4.1.13)$$

The resonance for the right wave occurs at $\omega = \omega_c$. The left wave has no resonance. The right wave has two pass bands (i.e., $n^2 > 0$) in the frequency bands $0 < \omega < \omega_c$ and $\omega > \omega_R$ separated by stop band (i.e., $n^2 < 0$), as shown clearly in the graph of n^2 versus ω , Fig. 4.1. The left wave has a pass band only for $\omega > \omega_L$.

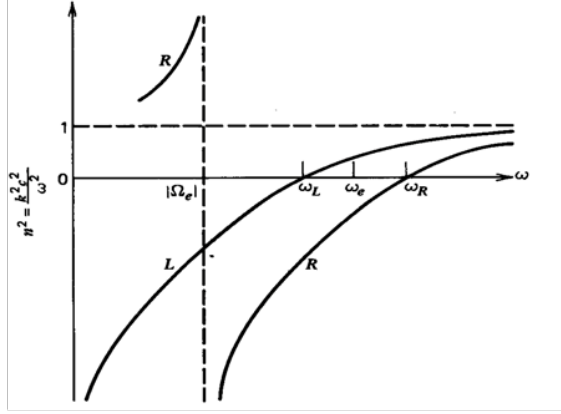


Figure 4.1: Dispersion graph for the parallel wave.[Reproduced from [23]]

4.1.2 Electromagnetic wave perpendicular to \mathbf{B}

Since the wave propagates perpendicular to \vec{B} , setting $n_x = n$ and $n_z = 0$ in Eq. (4.1.8), we get

$$\epsilon_1 E_x - i\epsilon_2 E_y = 0, \quad (4.1.14)$$

$$i\epsilon_2 E_x + (\epsilon_1 - n^2) E_y = 0, \quad (4.1.15)$$

$$(\epsilon_3 - n^2) E_z = 0. \quad (4.1.16)$$

Depending on the direction of the electric field relative to the magnetic field \vec{B} , two waves are defined: *the ordinary* and *the extraordinary* waves. *The ordinary wave* is the wave when the electric field is parallel to \vec{B} and *the extraordinary wave* is when the electric field is perpendicular to \vec{B} .

The ordinary wave

From (4.1.16), since $E_z \neq 0$, a nontrivial solution can be obtained if

$$\epsilon_3 - n^2 = 0,$$

$$n^2 = \epsilon_3,$$

$$n^2 = 1 - \frac{\omega_p^2}{\omega^2}, \quad (4.1.17)$$

which is the same dispersion equation as the unmagnetized plasma.

The extraordinary wave

From (4.1.14) and (4.1.15), since the electric component of the electromagnetic wave is in the xy -plane, the nontrivial solution can be obtained if

$$n^2 = \frac{(\epsilon_1^2 - \epsilon_2^2)}{\epsilon_1}. \quad (4.1.18)$$

Then, the dispersion relation is

$$n^2 = 1 - \frac{\omega_p^2(\omega^2 - \omega_p^2)}{\omega^2(\omega^2 - \omega_{UH}^2)} = \frac{(\omega^2 - \omega_L^2)(\omega^2 - \omega_R^2)}{\omega^2(\omega^2 - \omega_{UH}^2)}, \quad (4.1.19)$$

where $\omega_{UH}^2 = \omega_c^2 + \omega_p^2$, which is called *upper hybrid frequency*. From Eq (4.1.19) it is clear that the cutoff frequency is

$$\omega^2 = \frac{\omega_c}{2} + \omega_p^2 \pm \sqrt{\omega_p^2 + \frac{\omega_c^2}{4}},$$

or

$$\omega_{R/L} = \pm \frac{\omega_c}{2} + \sqrt{\omega_p^2 + \frac{\omega_c^2}{4}}. \quad (4.1.20)$$

That is, the cutoff occurs at $\omega = \omega_{R/L}$ and the resonance frequency is at $\omega = \omega_{UH}$, as shown in Fig. 4.2. Thus, the bands where there are no propagation for the ordinary wave lies in the range $0 < \omega < \omega_p$ and for the extraordinary wave $0 < \omega < \omega_L$ and $\omega_{UH} < \omega < \omega_R$, while the rest bands are pass bands.

4.2 Electromagnetic Waves in MPFG

To achieve a negative index material, it is customary to dissect the problem into two parts: a problem of negative permittivity and negative permeability.

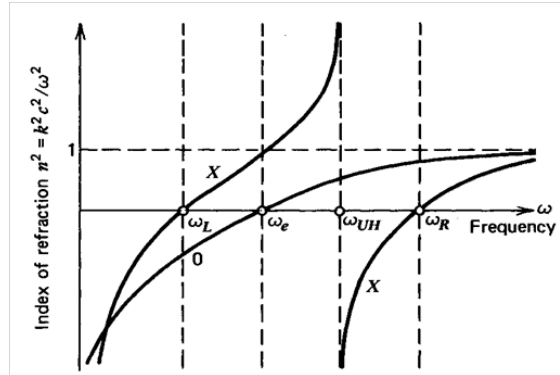


Figure 4.2: Dispersion graph for the perpendicular wave. [Reproduced from [23]]

As discussed in the previous section, in magnetized plasma there are ranges of frequencies in which the plasma is not transparent to electromagnetic waves. The existence of this “stop bands”, obviously, implies that the electric permittivity of the plasma in those ranges of frequencies is negative; which solves one part of the problem. Thus, roughly speaking, if negative permeability is introduced, by some means, within those bands of frequencies in which the magnetized plasma has negative permittivity, we will have negative refractive index media.

With this intuition we introduce tiny ferromagnetic grains in cold magnetized plasma as to enhance the magnetic activity. In this section we discuss the effects and the resulting expressions of the permeability tensor and the dispersion relation of MPFG.

4.2.1 The permeability tensor

Consider identical spherical ferromagnetic grains of radius a and N_g number density embedded uniformly in cold magnetized plasma in a constant strong magnetic field

H_0 . To avoid possible interference conductivity we shall use non metallic ferromagnets, ferrites. Under the influence of the external magnetic field H_0 directed along the z-axis, assumed the easy direction of the uniaxial ferromagnet, the magnetic dipoles of the ferromagnet align themselves. The static magnetization M_0 produced by the constant external magnetic field H_0 is $\sum \mu_m$. Applying a time varying weak magnetic field $\vec{H}(t) = \vec{H}'$ to this system results in a dispersion of the permeability tensor. Starting with the equation of motion

$$\frac{d\vec{M}}{dt} = \gamma(\vec{M} \times \vec{B}). \quad (4.2.1)$$

The equation of motion of the magnetization in a ferromagnet is [25],

$$\frac{d\vec{M}}{dt} = \gamma(\vec{H} + \beta M \hat{z}) \times \vec{M}, \quad (4.2.2)$$

where $\gamma = g|e|/2mc$, g is the gyromagnetic ratio, e and m are the charge and mass of an electron. $\beta > 0$ is the anisotropic coefficient.

With $\vec{H} = \vec{H}_0 + \vec{H}'$ and considering the varying components M_x and M_y due to \vec{H}' to be very small; and $M_z \approx M$ to be constant, we get

$$\begin{aligned} \frac{dM_x}{dt} &= \gamma H'_y M - \gamma(H_0 + \beta M)M_y, \\ \frac{dM_y}{dt} &= \gamma(H_0 + \beta M)M_x - \gamma H'_x M. \end{aligned}$$

With time dependency $e^{-i\omega t}$, the above relation yields

$$\begin{aligned} -i\omega M_x &= \gamma H'_y M - \gamma(H_0 + \beta M)M_y, \\ -i\omega M_y &= \gamma(H_0 + \beta M)M_x - \gamma H'_x M. \end{aligned}$$

Using $\omega_H = \gamma H_0$ and $\omega_m = \gamma \beta M$, we get

$$\begin{aligned} -i\omega M_x &= \frac{\omega_m}{\beta} H'_y - (\omega_m + \omega_H)M_y, \\ -i\omega M_y &= (\omega_m + \omega_H)M_x - \frac{\omega_m}{\beta} H'_x. \end{aligned}$$

Solving these two equations yields

$$M_x = \frac{\omega_m}{\beta} \frac{(\omega_H + \omega_m)}{[(\omega_H + \omega_m)^2 - \omega^2]} H'_x - \frac{i\omega\omega_m}{\beta[(\omega_H + \omega_m)^2 - \omega^2]} H'_y, \quad (4.2.3)$$

$$M_y = \frac{i\omega\omega_m}{\beta[(\omega_H + \omega_m)^2 - \omega^2]} H'_x + \frac{\omega_m}{\beta} \frac{(\omega_H + \omega_m)}{[(\omega_H + \omega_m)^2 - \omega^2]} H'_y. \quad (4.2.4)$$

Since $M = \chi H$, the coefficients in equations (4.2.3) and (4.2.4) are the components of the magnetic susceptibility tensor. The nonzero components of the susceptibility tensor are

$$\chi_{xx} = \chi_{yy} = \frac{\omega_m}{\beta} \frac{(\omega_H + \omega_m)}{[(\omega_H + \omega_m)^2 - \omega^2]}, \quad (4.2.5)$$

$$\chi_{xy} = -\chi_{yx} = \frac{i\omega\omega_m}{\beta[(\omega_H + \omega_m)^2 - \omega^2]}. \quad (4.2.6)$$

Using the relation

$$\mu_{ij} = \delta_{ij} + 4\pi\nu N_g \chi_{ij}$$

, where $\nu = \frac{4}{3}\pi a^3$ is the volume the grains, and in the limit $\beta \rightarrow 0$, the components of the permeability tensor are

$$\mu_{xx} = \mu_{yy} = 1 - \nu N_g \frac{\omega_H \omega_M}{\omega^2 - \omega_H^2} = \mu_1, \quad (4.2.7)$$

$$\mu_{xy} = -\mu_{yx} = \nu N_g \frac{\omega \omega_M}{\omega^2 - \omega_H^2} = \mu_2, \quad (4.2.8)$$

$$\mu_{zz} = \mu_3 = 1, \quad (4.2.9)$$

where $\omega_M = 4\pi\gamma M$.

4.2.2 The dispersion relation

Consider a high frequency plane electromagnetic wave $\sim e^{(i\vec{k}\cdot\vec{x} - i\omega t)}$ in the xz -plane and the external magnetic field $\vec{H} = H_0 \hat{z}$. Applying the Maxwell's equations we obtain

$$\vec{k} \times \vec{E} = \omega \mu_0 \bar{\mu} \vec{H} \quad (4.2.10)$$

$$\vec{k} \times \vec{H} = -\omega \epsilon_0 \bar{\epsilon} \vec{E} \quad (4.2.11)$$

From Eq. (4.2.10) with the permeability tensor

$$\bar{\mu} = \begin{pmatrix} \mu_1 & i\mu_2 & 0 \\ -i\mu_2 & \mu_1 & 0 \\ 0 & 0 & \mu_3 \end{pmatrix}, \quad (4.2.12)$$

we get

$$\begin{aligned} -k_z E_y &= \omega\mu_0\mu_1 H_x + i\omega\mu_0\mu_2 H_y, \\ k_z E_x - k_x E_z &= -i\omega\mu_0\mu_2 H_x + \omega\mu_0\mu_1 H_y, \\ k_x E_y &= \omega\mu_0\mu_3 H_z. \end{aligned} \quad (4.2.13)$$

And, from Eq. (4.2.11) with the permittivity tensor

$$\bar{\epsilon} = \begin{pmatrix} \epsilon_1 & i\epsilon_2 & 0 \\ -i\epsilon_2 & \epsilon_1 & 0 \\ 0 & 0 & \epsilon_3 \end{pmatrix}, \quad (4.2.14)$$

where

$$\epsilon_1 = 1 - \frac{\omega_p^2}{\omega^2 - \omega_c^2}, \quad \epsilon_2 = \frac{\omega_c \omega_p^2}{\omega(\omega^2 - \omega_c^2)}, \quad \epsilon_3 = 1 - \frac{\omega_p^2}{\omega^2},$$

we get

$$\begin{aligned} k_z H_y &= \omega\epsilon_0\epsilon_1 E_x + i\omega\epsilon_0\epsilon_2 E_y, \\ k_z H_x - k_x H_z &= i\omega\epsilon_0\epsilon_2 E_x - \omega\epsilon_0\epsilon_1 E_y, \\ k_x H_y &= -\omega\epsilon_0\epsilon_3 E_z. \end{aligned} \quad (4.2.15)$$

From (4.2.13), the components of the magnetic field can be expressed as

$$\begin{aligned} H_x &= \frac{1}{\omega\mu_0\Delta_2} (-i\mu_2 k_z E_x - \mu_1 k_z E_y + i\mu_2 k_x E_z), \\ H_y &= \frac{1}{\omega\mu_0\Delta_2} (\mu_1 k_z E_x - i\mu_2 k_z E_y - \mu_1 k_x E_z), \\ H_z &= \frac{k_x E_y}{\omega\mu_0\mu_3}, \end{aligned} \quad (4.2.16)$$

where $\Delta_2 = \mu_1^2 - \mu_2^2$

From (4.2.15), we have

$$\begin{aligned} E_x &= \frac{1}{\omega\epsilon_0\Delta_1}(i\epsilon_2k_zH_x + \epsilon_1k_zH_y - i\epsilon_2k_xH_z), \\ E_y &= \frac{1}{\omega\epsilon_0\Delta_1}(-\epsilon_1k_zH_x + i\epsilon_2k_zH_y + \epsilon_1k_xH_z), \\ E_z &= -\frac{k_xH_y}{\omega\epsilon_0\epsilon_3}, \end{aligned} \quad (4.2.17)$$

where $\Delta_1 = \epsilon_1^2 - \epsilon_2^2$.

Substituting the respective expressions of H in (4.2.16) into (4.2.17), yields three linear equations in E , which can be expressed in matrix form as

$$\begin{pmatrix} \left(\frac{an_z^2}{\Delta_1\Delta_2} - 1\right) & -i\left(\frac{bn_z^2}{\Delta_1\Delta_2} + \frac{\epsilon_2n_x^2}{\Delta_1\mu_3}\right) & -\frac{an_xn_z}{\Delta_1\Delta_2} \\ i\frac{bn_z^2}{\Delta_1\Delta_2} & \left(\frac{an_z^2}{\Delta_1\Delta_2} + \frac{\epsilon_1n_x^2}{\Delta_1\mu_3} - 1\right) & -i\frac{bn_xn_z}{\Delta_1\Delta_2} \\ -\frac{\mu_1n_xn_z}{\epsilon_3\Delta_2} & i\frac{\mu_2n_xn_z}{\epsilon_3\Delta_2} & \left(\frac{\mu_1n_x^2}{\epsilon_3\Delta_2} - 1\right) \end{pmatrix} \begin{pmatrix} E_x \\ E_y \\ E_z \end{pmatrix} = 0, \quad (4.2.18)$$

where the index of refraction $n = (ck)/\omega$ and $\vec{n} = n_x\hat{x} + n_z\hat{z} = n\sin\theta\hat{x} + n\cos\theta\hat{z}$, where θ is the angle between the direction of the electromagnetic wave and the magnetic field. In (4.2.18), $a = \epsilon_1\mu_1 + \epsilon_2\mu_2$ and $b = \epsilon_1\mu_2 + \epsilon_2\mu_1$.

From equation (4.2.18), the dispersion relation can be obtained by equating the determinant to zero. The dispersion relation that we obtain from matrix equation (4.2.18) will, obviously, be a function of the angle θ , $n = n(\omega, \theta)$. That is, the dispersion equation is

$$\begin{aligned} &[\mu_3 \cos^2 \theta (\epsilon_3 \cos^2 \theta + \epsilon_1 \sin^2 \theta) + \mu_1 \sin^2 \theta (\epsilon_3 \cos^2 \theta + \epsilon_1 \sin^2 \theta)] n^4 \\ &- [2\epsilon_3\mu_3 \cos^2 \theta (\epsilon_1\mu_1 + \epsilon_2\mu_2) + (\mu_1\mu_3\Delta_1 + \epsilon_1\epsilon_3\Delta_2) \sin^2 \theta] n^2 \\ &+ \epsilon_3\mu_3\Delta_1\Delta_2 = 0. \end{aligned} \quad (4.2.19)$$

This is a quadratic equation in the square of the index of refraction. Now, depending on the direction of the electromagnetic wave relative to the constant external magnetic field $\vec{H} = H_0\hat{z}$, we may consider the dispersion relation of two cases.

Electromagnetic Wave Parallel to $\vec{H} = H_0 \hat{z}$

Since the electromagnetic wave is in the z -direction, setting $n_x = 0$ and $n_z = n$, in equation (4.2.18), yields

$$\begin{aligned} \left(\frac{an^2}{\Delta_1 \Delta_2} - 1 \right) E_x - i \frac{bn^2}{\Delta_1 \Delta_2} E_y &= 0, \\ i \frac{bn^2}{\Delta_1 \Delta_2} E_x + \left(\frac{an^2}{\Delta_1 \Delta_2} - 1 \right) E_y &= 0, \\ (-E_z) &= 0. \end{aligned} \quad (4.2.20)$$

In (4.2.20), the third equation, obviously, implies that $E_z = 0$. From the first two equations, we get

$$\frac{iE_x}{E_y} = -\frac{bn^2}{an^2 - \Delta_1 \Delta_2} = -\frac{an^2 - \Delta_1 \Delta_2}{bn^2}. \quad (4.2.21)$$

This implies that the x - and y -components of the electric field are circularly polarized.

The dispersion relation is

$$\begin{aligned} (an^2 - \Delta_1 \Delta_2)^2 &= (bn^2)^2, \\ n^2(\omega, 0) &= \frac{\Delta_1 \Delta_2}{a \pm b}, \\ n^2(\omega, 0) &= (\epsilon_1 \pm \epsilon_2)(\mu_1 \pm \mu_2). \end{aligned} \quad (4.2.22)$$

Equation (4.2.22) indicates that there are two waves with refractive index

$$n_+^2(\omega, 0) = \left(1 - \frac{\omega_p^2}{\omega(\omega + \omega_c)} \right) \left(1 + \frac{\xi \omega_M}{(\omega + \omega_c)} \right), \quad (4.2.23)$$

$$n_-^2(\omega, 0) = \left(1 - \frac{\omega_p^2}{\omega(\omega - \omega_c)} \right) \left(1 - \frac{\xi \omega_M}{(\omega - \omega_c)} \right), \quad (4.2.24)$$

where $\xi = \nu N_g$ and $\omega_H \approx \omega_c$. The "±" represent the left and right waves, respectively.

For the sake of clarity, let's write equations (4.2.23) and (4.2.24) as

$$n_+ = \epsilon_+ \mu_+ \quad n_- = \epsilon_- \mu_-$$

A medium would be taken as LHM only if both ϵ and μ are simultaneously negative.

But as it is seen in (4.2.23), μ_+ is always positive. Hence, no possibilities of the right

wave to have a negative refractive index. On the other hand, the left wave, for the short frequency range $\omega_c < \omega < \omega_p$, there is a possibility of both ϵ_- and μ_- having negative value simultaneously.

Electromagnetic Wave Perpendicular to $\vec{H} = H_0 \hat{z}$

Here the electromagnetic wave is in the x -direction. Thus, in (4.2.18), setting $n_z = 0$ and $n_x = n$, we get

$$\begin{aligned} -E_x - i \left(\frac{\epsilon_2 n_x^2}{\Delta_1 \mu_3} \right) E_y &= 0, \\ \left(\frac{\epsilon_1 n_x^2}{\Delta_1 \mu_3} - 1 \right) E_y &= 0, \\ \left(\frac{\mu_1 n_x^2}{\epsilon_3 \Delta_2} - 1 \right) &= 0. \end{aligned} \quad (4.2.25)$$

There are two cases: the electric field parallel and perpendicular to the external magnetic field, the ordinary and the extraordinary waves, respectively.

The ordinary wave:

From (4.2.25), the nontrivial solution to the third equation yields

$$n^2(\omega, \pi/2) = \frac{\epsilon_3 \Delta_2}{\mu_1} = \frac{\epsilon_3 (\mu_1^2 - \mu_2^2)}{\mu_1}, \quad (4.2.26)$$

which reduces to the dispersion equation of magnetized plasma if $\mu_1 = 1$ and if $\mu_2 = 0$.

Equation (4.2.26) in terms of the components is

$$n^2(\omega, \pi/2) = \left(1 - \frac{\omega_p^2}{\omega^2} \right) \left(1 - \frac{\xi \omega_M (\xi \omega_M - \omega_c)}{\omega^2 - \omega_c (\xi \omega_M - \omega_c)} \right). \quad (4.2.27)$$

We can rewrite equation (4.2.27) as $n^2 = \epsilon \mu$, where

$$\epsilon = \left(1 - \frac{\omega_p^2}{\omega^2} \right),$$

and

$$\mu = \left(1 - \frac{\xi \omega_M (\xi \omega_M - \omega_c)}{\omega^2 - \omega_c (\xi \omega_M - \omega_c)} \right).$$

The extraordinary wave:

Considering the second equation in Eq. (4.2.25) we get the dispersion relation as

$$n^2(\omega, \pi/2) = \frac{\mu_3 \Delta_1}{\epsilon_1} = \frac{\mu_3(\epsilon_1^2 - \epsilon_2^2)}{\epsilon_1}. \quad (4.2.28)$$

This is the same equation as that of the extraordinary wave in magnetized plasma, except that here the magnetic permeability μ_3 is included. Since $\mu_3 = 1$, negative index of refraction cannot be attained.

From the above discussion there are two cases in which the MPFG media behaves as a left-handed media. The dispersion equations of these two cases are

$$n_-^2(\omega, 0) = \left(1 - \frac{\omega_p^2}{\omega(\omega - \omega_c)}\right) \left(1 - \frac{\xi\omega_M}{(\omega - \omega_c)}\right),$$

and

$$n^2(\omega, \frac{\pi}{2}) = \left(1 - \frac{\omega_p^2}{\omega^2}\right) \left(1 - \frac{\xi\omega_M(\xi\omega_M + \omega_c)}{\omega^2 - \omega_c(\xi\omega_M + \omega_c)}\right).$$

In both cases the range of frequency, $\Delta\omega$, in which the MPFG behaves as a LHM depends on the resonance frequency, $\xi\omega_M$, of the ferromagnetic subsystem. Specifically, the MPFG will have negative refractive index in the range of frequency equal to $\Delta\omega \sim \xi\omega_M = 4\pi\nu N_g \gamma M$. This implies that the range of frequency in which the MPFG acts as LHM also depends on the magnetization of the ferromagnetic grains. On the other hand the magnetization of the ferromagnetic grains should be very small compared to the external static magnetic field in order to avoid dipole-dipole interaction. That is, $4\pi\nu N_g M \ll H_0$ which leads to $4\pi\nu N_g \gamma M \ll \gamma H_0$ which implies $\xi\omega_M \ll \omega_H \sim \omega_c$ and thus $\xi\omega_M/\omega_c \ll 1$ and $4\pi\nu N_g \chi \ll 1$. For a plasma with ferromagnetic grains $a \sim 10^{-4} \text{cm}$ and $N_g \sim 10^6$, $\nu N_g \ll 1$.

Introducing the following unit-less frequency representation

$$x = \frac{\omega}{\omega_c}, \quad x_p = \frac{\omega_p}{\omega_c}, \quad x_m = \frac{\xi\omega_M}{\omega_c},$$

the above two equations of the index of refraction can be written as

$$n_-^2(\omega, 0) = \left(1 - \frac{x_p^2}{x(x-1)}\right) \left(1 - \frac{x_m}{(x-1)}\right), \quad (4.2.29)$$

$$n^2(\omega, \pi/2) = \left(1 - \frac{x_p^2}{x^2}\right) \left(1 - \frac{x_m(x_m+1)}{x^2 - (x_m+1)}\right). \quad (4.2.30)$$

As discussed above, the magnetization of the ferromagnetic grains and hence the resonance frequency is the essential factor for the MPFG to behave as a LHM. This dependency can be verified from the graphs of the index of refraction versus the reduced frequency and the graphs of the permittivity/permeability versus the reduced frequency drawn for fixed value of $x_p = 1.1$ and different values of x_m .

First let's consider the case when the wave is parallel to the constant magnetic field. For $x_p = 1.1$, the permittivity is negative for $1 < x < 1.708$, as shown in Fig. 4.3.

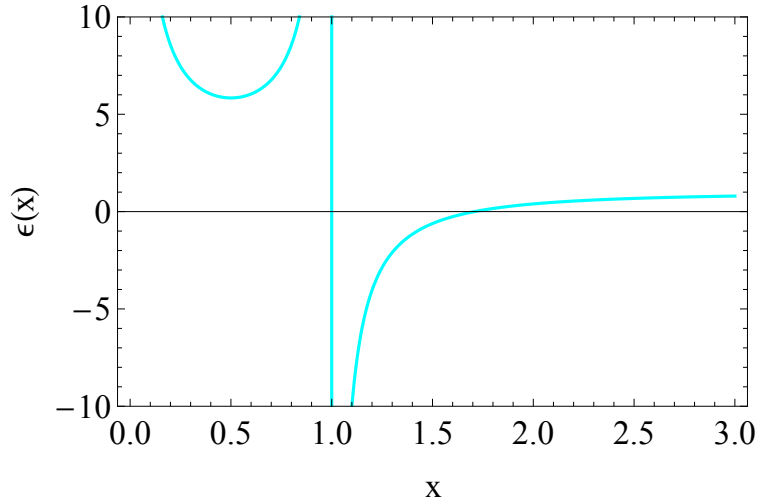


Figure 4.3: The permittivity (ϵ) as a function of the dimensionless frequency x for the parallel propagation with $x_p = 1.1$.

The permeability, $n^2(\omega, 0)$ and $n(\omega, 0)$ graphs for $x_m = 0.06, 0.08$ and 0.5 , shown on Fig. 4.4, substantiate the fact that the range of frequency in which the MPFG

Table 4.1: The different ranges of frequencies where the MPFG is RHM, LHM or nontransparent when the wave is parallel.

x	ϵ	μ	n^2	n
$0 < x < 1$	+	+	RHM	RHM
$1 < x < x_m + 1$	-	-	LHM	LHM
$x = x_m + 1$	-	0	0	0
$x_m + 1 < x < \frac{1 + \sqrt{1 + 4x_p^2}}{2}$	-	+	-	No
$x = \frac{1 + \sqrt{1 + 4x_p^2}}{2}$	0	+	0	0
$x > \frac{1 + \sqrt{1 + 4x_p^2}}{2}$	+	+	RHM	RHM

behaves as LHM depends on the grains magnetization resonance frequency.

From Fig. 4.4, 4.5 and 4.6 we see that the permeability is negative only in the range $1 < x < x_m + 1$ and this is the range in which the MPFG is LHM. This range can be increased by increasing x_m . Table 4.1, summarizes the dependency of the constitutive parameters on the frequency of the electromagnetic wave. From Table 4.1, we can see that had it been possible to increase x_m to a value $x_m = (-1 + \sqrt{1 + 4x_p^2})/2 \simeq 0.708$ the MPFG media would be transparent for the parallel electromagnetic wave, regardless of the frequency of the wave, as shown in Fig. 4.11. But as it is stated $x_m = (\xi\omega_M)/\omega_c \ll 1$.

Similarly, consider the case when the wave is perpendicular to the constant magnetic field. For $x_p = 1.1$, the permittivity is negative for $0 < x < 1.1$, Fig. 4.7.

The permeability, $n^2(\omega, \pi/2)$ and $n(\omega, \pi/2)$ graphs for $x_m = 0.06, 0.08$ and 0.1 , shown below, substantiate the fact that the range of frequency in which the MPFG behaves as LHM depends on the grains magnetization resonance frequency.

From Fig. 4.10 we see that the permeability is negative only in the range $\sqrt{x_m + 1} < x < x_m + 1$ (or in the range $\sqrt{x_m + 1} < x < x_p$ if $x_p < x_m + 1$) and this is the range

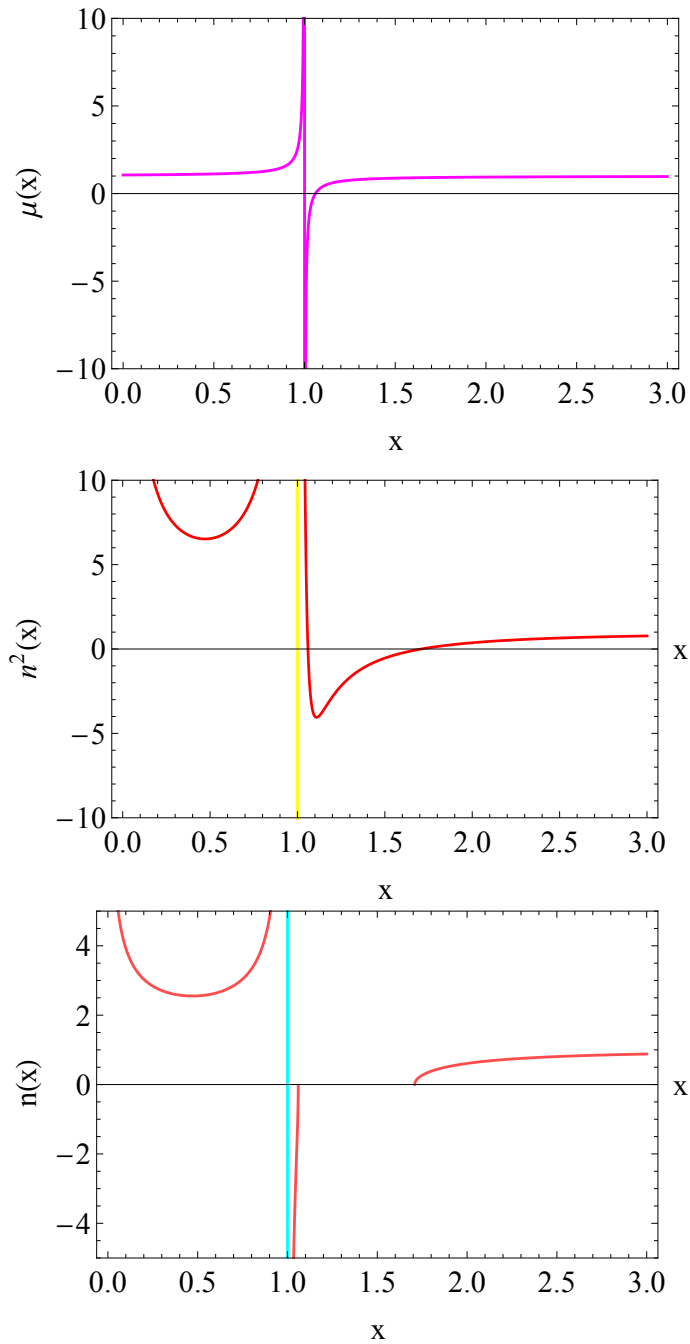


Figure 4.4: The permeability (μ), n^2 , and n versus x for parallel propagation with $x_m = 0.06$.

These graphs shows that μ is negative only in the range $1 < x < 1.06$ and within this range the MPFG is LHM ;and the width of this range is $\Delta x = 0.06$.

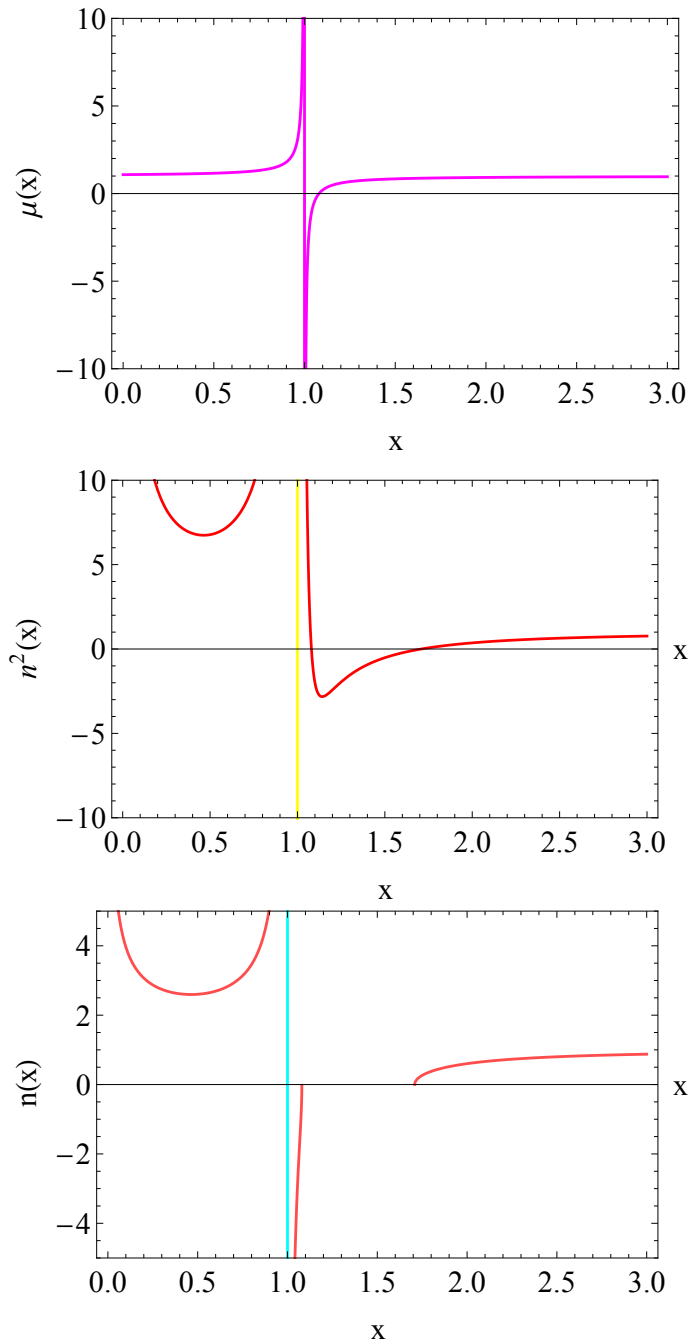


Figure 4.5: The permeability (μ), n^2 , and n versus x for parallel propagation with $x_m = 0.08$.

These graphs shows that μ is negative only in the range $1 < x < 1.08$ and within this range the MPFG is LHM ;and the width of this range is $\Delta x = 0.08$.

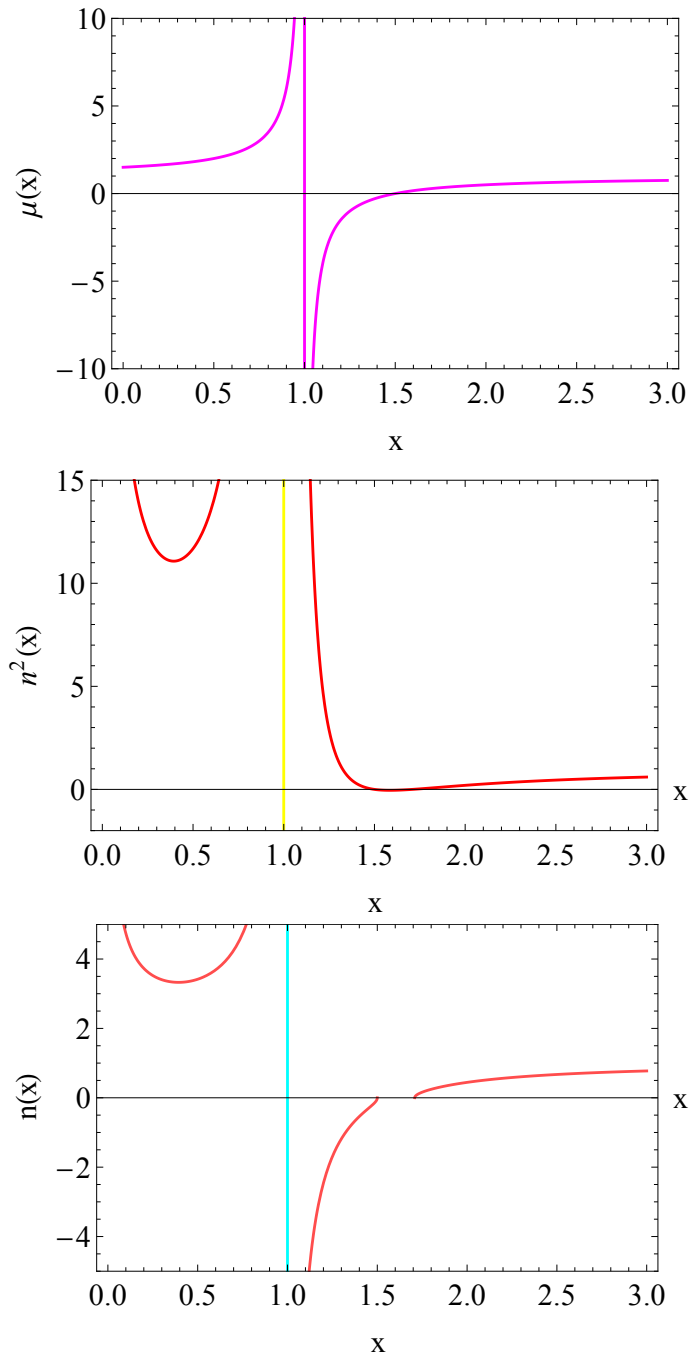


Figure 4.6: The permeability (μ), n^2 , and n versus x for parallel propagation with $x_m = 0.5$.

These graphs shows that μ is negative only in the range $1 < x < 1.5$ and within this range the MPFG is LHM ;and the width of this range is $\Delta x = 0.5$.

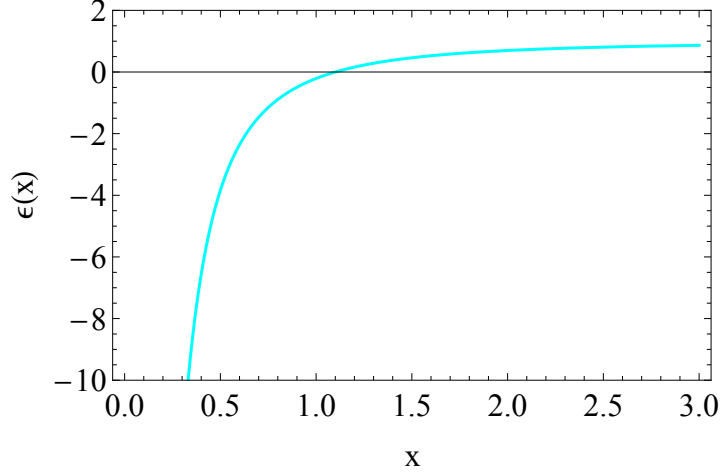


Figure 4.7: The permittivity (ϵ) as a function of the dimensionless frequency x for the perpendicular propagation with $x_p = 1.1$.

in which the MPFG is LHM. This range increases as the value of x_m increased. Table 4.2, summarizes the range in which the MPFG behaves as RHM, LHM and not transparent. From Table 4.2 it can be seen that if it were possible to increase x_m to a value $x_m = x_p - 1 = 0.1$ the MPFG media would be transparent for the perpendicular electromagnetic wave at every frequency of the wave, as shown in Fig. 4.11. However, $x_m \ll 1$ as indicated in the above discussion.

From the two sets of graphs we may observe that for the same increase of the value of x_m the range of frequency within which the MPFG acts as LHM is greater when the wave is parallel to the external applied magnetic field than when it is perpendicular. Besides the value of x_m can be increased to a larger value for the parallel wave (in this case up to ~ 0.708) compared to the perpendicular wave (up to ~ 0.1).

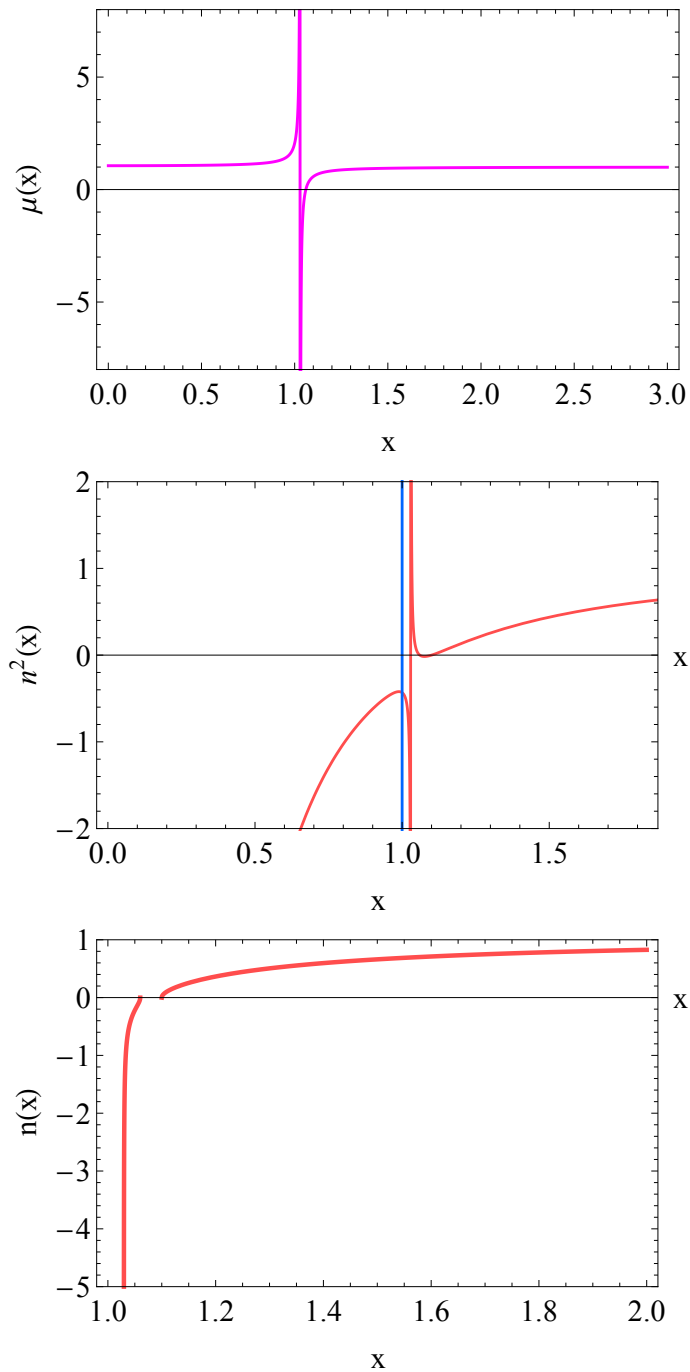


Figure 4.8: The permeability (μ), n^2 , and n versus x for perpendicular propagation with $x_m = 0.06$.

These graphs shows that μ is negative only in the range $1.03 < x < 1.06$ and within this range the MPFG is LHM ;and the width of this range is $\Delta x = 0.03$.

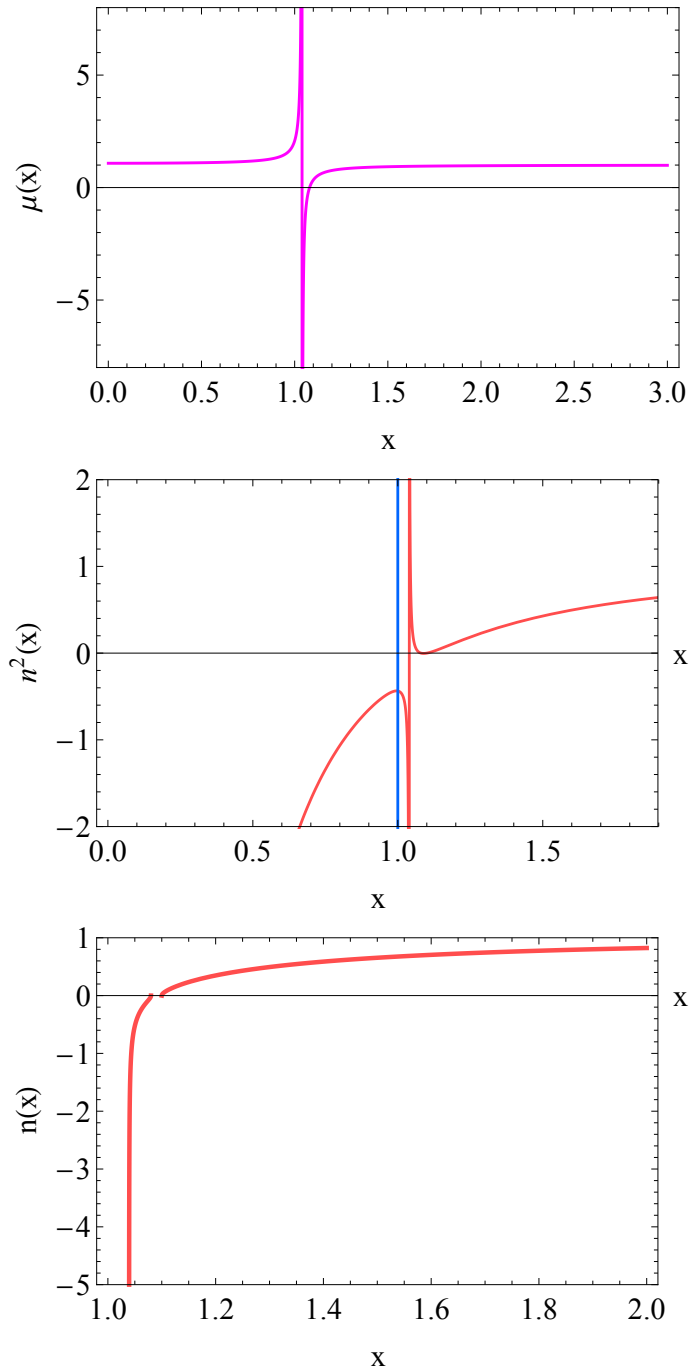


Figure 4.9: The permeability (μ), n^2 , and n versus x for perpendicular propagation with $x_m = 0.08$.

These graphs shows that μ is negative only in the range $1.04 < x < 1.08$ and within this range the MPFG is LHM ;and the width of this range is $\Delta x = 0.04$.

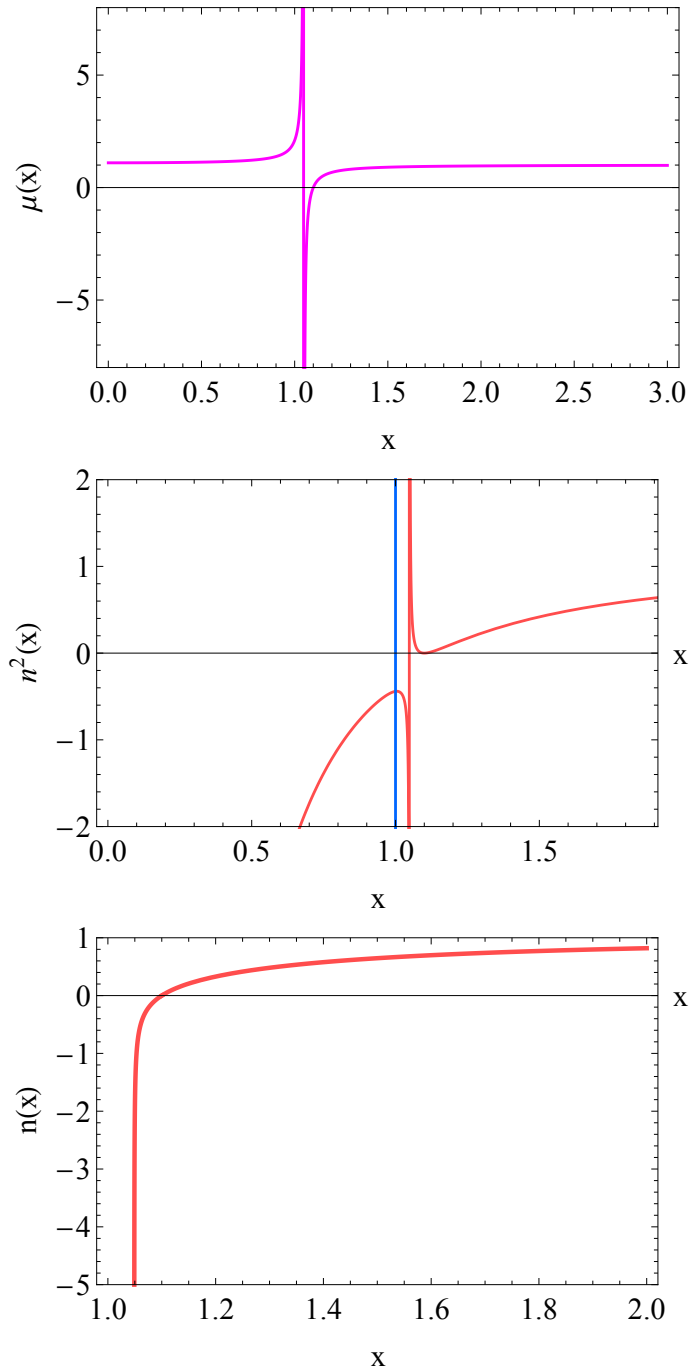


Figure 4.10: The permeability (μ), n^2 , and n versus x for perpendicular propagation with $x_m = 0.1$.

These graphs shows that μ is negative only in the range $1.05 < x < 1.1$ and within this range the MPFG is LHM ;and the width of this range is $\Delta x = 0.05$.

Table 4.2: The different ranges of frequencies where the MPFG is RHM, LHM or nontransparent when the wave is perpendicular.

x	ϵ	μ	$n^2(\omega, \frac{\pi}{2})$	$n(\omega, \frac{\pi}{2})$
$0 < x < \sqrt{x_m + 1}$	-	+	-	No
$x = \sqrt{x_m + 1}$	-	0	0	0
$\sqrt{x_m + 1} < x < x_m + 1$	-	-	LHM	LHM
$x = x_m + 1$	-	0	0	0
$x_m + 1 < x < x_p$	-	+	-	No
$x = x_p$	0	+	0	0
$x > x_p$	+	+	RHM	RHM

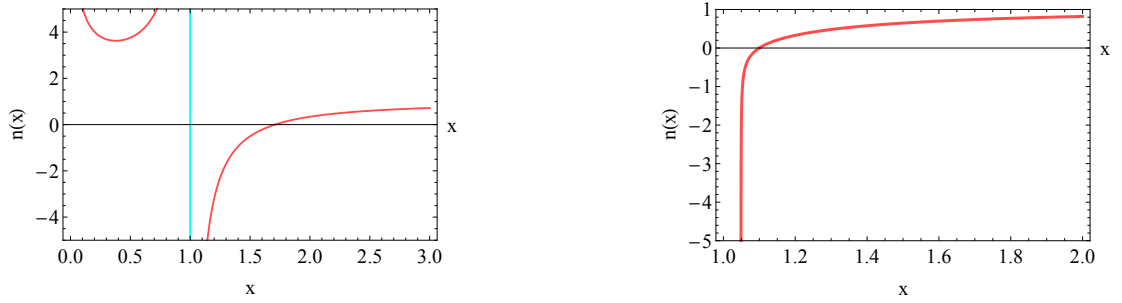


Figure 4.11: (Left) n versus x graph for the parallel wave at $x_m = 0.708$. (Right) n versus x graph for the perpendicular wave at $x_m = 0.1$.

4.3 Phase velocity, group velocity and energy flow in MPFG

The phase velocity, \vec{v}_{ph} and the group velocity, \vec{v}_g are given by

$$v_{ph} = \frac{\omega}{k} \qquad v_g = \frac{d\omega}{dk}$$

For the parallel wave, the phase velocity in the MPFG can be given as

$$v_p = \frac{c}{n} = \frac{c}{\sqrt{\left(1 - \frac{\omega_p^2}{\omega(\omega - \omega_c)}\right) \left(1 - \frac{\xi\omega_M}{(\omega - \omega_c)}\right)}}$$

$$v_p = \frac{c}{\sqrt{\left(1 - \frac{x_p^2}{x(x-1)}\right) \left(1 - \frac{x_m}{(x-1)}\right)}}$$
(4.3.1)

Using Eq. (2.1.18), the group velocity is

$$v_g = \frac{2c(-1+x)^3x\sqrt{\left(1 - \frac{x_p^2}{x(x-1)}\right) \left(1 - \frac{x_m}{(x-1)}\right)}}{-(1+x_m)x_p^2 + (x_p^2 - x_mx_p^2 - 2x_m - 2)x + (6 + 3x_m)x^2 - (x_m + 6)x^3 + 2x^4}$$
(4.3.2)

In a negative refractive index material the phase and group velocity are antiparallel. This can be deduced from the graph of the phase and group velocity against the reduced frequency drawn for $x_m = 0.5$, as shown in Fig. 4.12. From the graph we see that in the range of frequency $1 < x < 1.5$ the phase velocity and the group velocity are of opposite sign indicating that in this region the MPFG actually is a LHM. The graph also shows that as the frequency approaches higher values the phase and group velocities converge to the same value-the speed of light in free space, c .

Similarly, the phase velocity for the perpendicular wave is

$$v_p = \frac{c}{n} = \frac{c}{\sqrt{\left(1 - \frac{\omega_p^2}{\omega^2}\right) \left(1 - \frac{\xi\omega_M(\xi\omega_M + \omega_c)}{(\omega^2 - \omega_c(\xi\omega_M + \omega_c))}\right)}}$$

$$v_p = \frac{c}{\sqrt{\left(1 - \frac{x_p^2}{x^2}\right) \left(1 - \frac{x_m(x_m+1)}{(x^2 - (x_m+1))}\right)}}$$
(4.3.3)

and the group velocity is

$$v_g = \frac{c(x^2 - (1+x_m))^2\sqrt{\left(1 - \frac{x_p^2}{x^2}\right) \left(1 - \frac{x_m(x_m+1)}{(x^2 - (x_m+1))}\right)}}{(x^2 - (1+x_m))^2 + x_m(x_m+1)^2 - x_m(x_m+1)x_p^2}$$
(4.3.4)

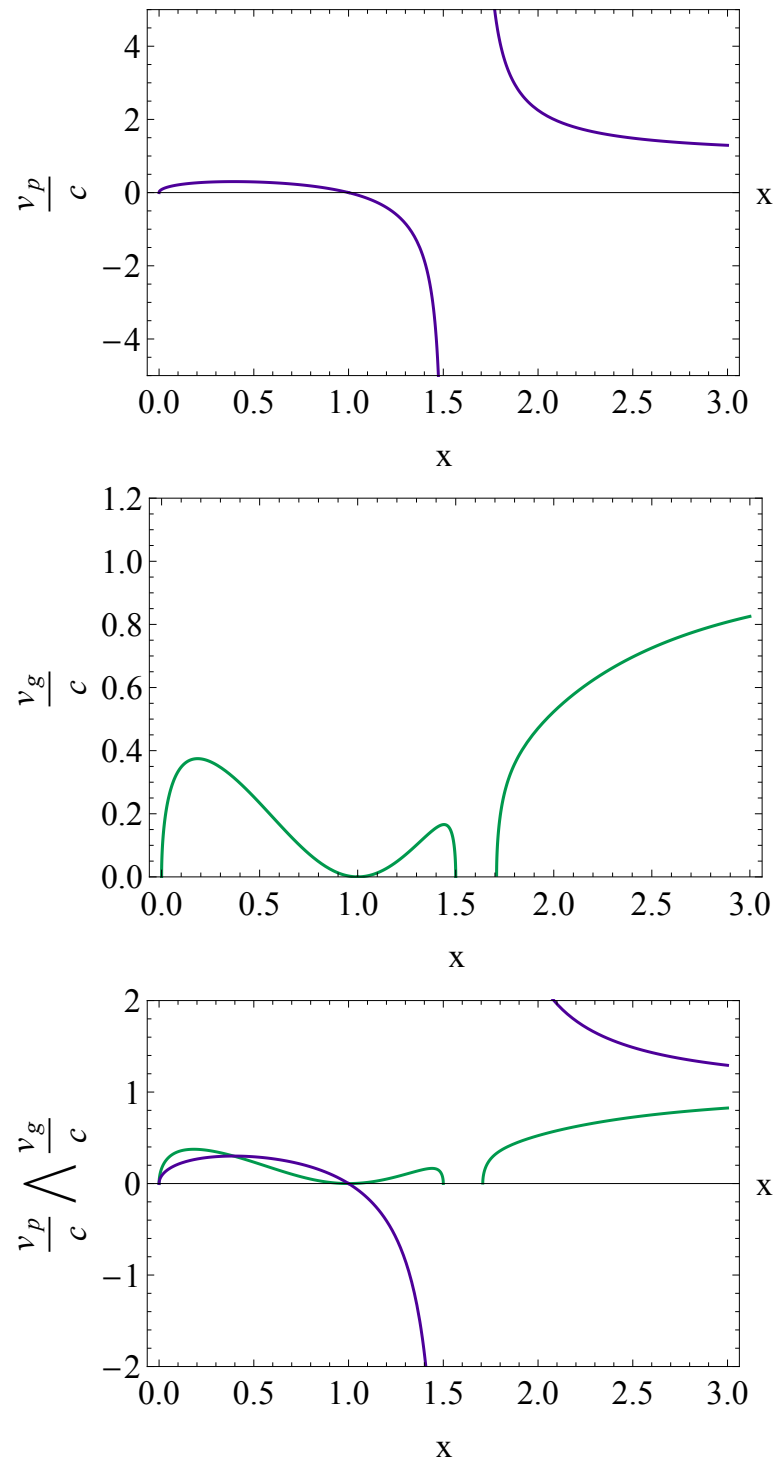


Figure 4.12: The normalized phase velocity $\frac{v_p}{c}$, the normalized group velocity $\frac{v_g}{c}$ and the normalized phase and group velocity combined, respectively, graph for the parallel wave at $x_m = 0.5$.

The graph of the phase and group velocity against the unit less frequency, Fig. 4.13, verifies that, for $x_m = 0.08$, in the range $1.04 < x < 1.1$, where the MPFG behaves as LHM, the phase and group velocity are antiparallel.

The Poynting vector given by

$$\vec{S} = \frac{c}{8\pi} \text{Re}(\vec{E} \times \vec{H}^*)$$

can be expressed in terms of \vec{E} as

$$S = \frac{c}{8\pi} \frac{n}{\mu} E^2$$

. Considering the parallel and the perpendicular wave the energy flow is

$$S_z(0) = \frac{c}{8\pi} \frac{n_-(\omega, 0)}{\mu_1 - \mu_2} E^2 \quad (4.3.5)$$

$$S(\frac{\pi}{2}) = \frac{c}{8\pi} \frac{\mu_1 n_-(\omega, \frac{\pi}{2})}{\mu_1^2 - \mu_2^2} E^2 \quad (4.3.6)$$

Since $S > 0$, in the range of frequency in which the MPFG acts as a LHM, for $S(0) > 0$ to be true the permeability $\mu_1 - \mu_2 < 0$ and for $S(\frac{\pi}{2}) > 0$ to be true $\frac{\mu_1^2 - \mu_2^2}{\mu_1} < 0$. Expressing the above equations in terms of the phase velocity

$$S_z(0) = \frac{c^2}{8\pi} \frac{1}{(\mu_1 - \mu_2)v_p} E^2$$

and

$$S(\frac{\pi}{2}) = \frac{c^2}{8\pi} \frac{\mu_1}{(\mu_1^2 - \mu_2^2)v_p} E^2.$$

In other words, the product of the phase velocity and the energy flow, in the range of frequency where the MPFG is LHM, is negative, i.e.,

$$S_z(0)v_p < 0,$$

which implies that the phase velocity is oppositely directed to the energy flow.

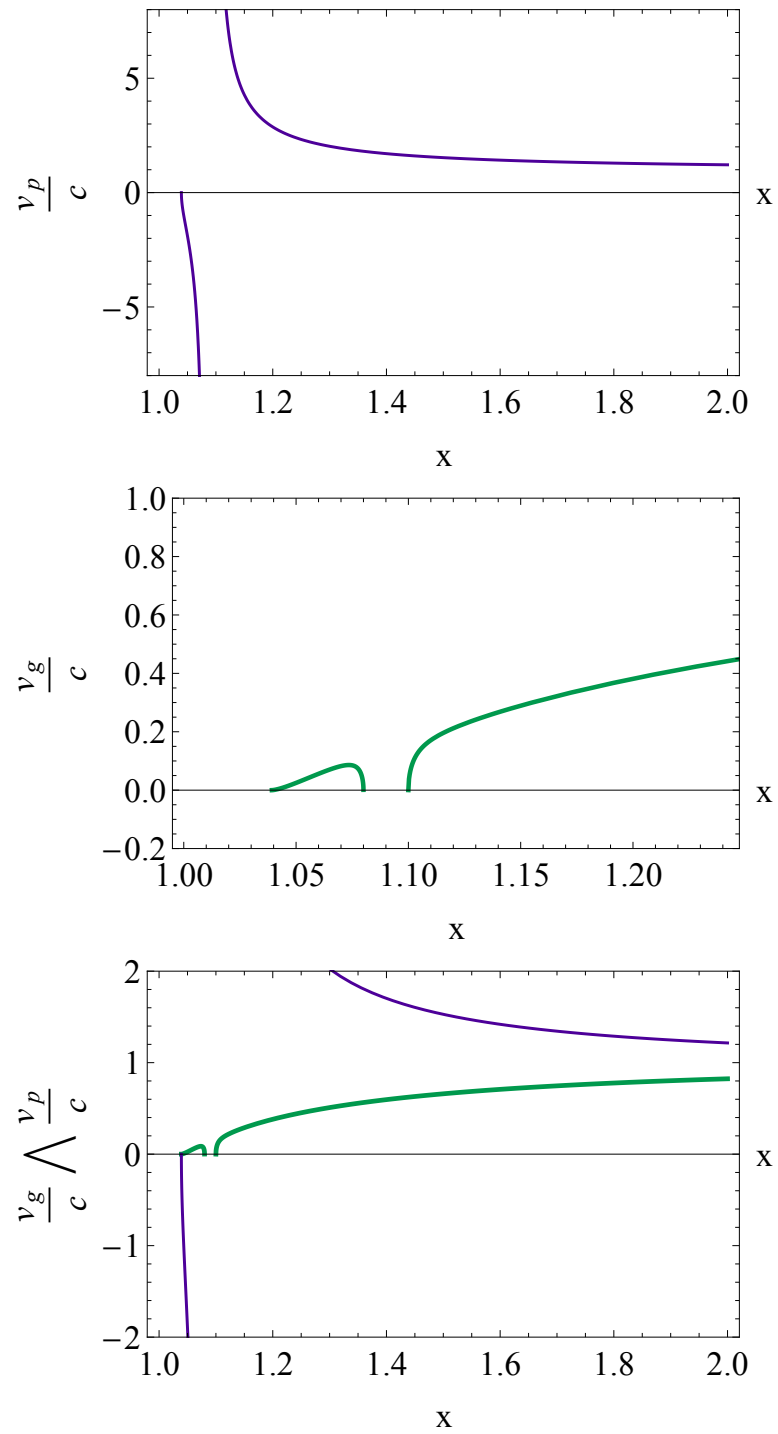


Figure 4.13: The normalized phase velocity $\frac{v_p}{c}$, the normalized group velocity $\frac{v_g}{c}$ and the normalized phase and group velocity combined, respectively, graph for the perpendicular wave at $x_m = 0.08$.

Chapter 5

Conclusion

A medium would be taken as LHM only if both ϵ and μ are simultaneously negative. From the discussions in Section 4.1, it is obvious that the conventional magnetized plasma have a negative permittivity in different frequency ranges depending upon the direction of the electromagnetic wave relative to the direction applied magnetic field. In these ranges of frequency the magnetized plasma is nontransparent to electromagnetic waves. This implies that the magnetized plasma to be transparent in these ranges, the permeability in these ranges should be negative. In the thesis we studied the mechanism of enhancing the magnetic activity by embedding magnetically active materials such as ferromagnetic materials in the magnetized plasma. The result obtained clearly shows that for the range of frequency in which the MPFG behaves as a LHM, the plasma frequency strongly depends on the magnetic resonance frequency, ω_M of the ferromagnetic grains. As the ω_M increased the range of frequency for which the MPFG is LHM also increases. As it is expected, within this range, the phase velocity and the group velocity are anti parallel.

Moreover, the MPFG media is tunable in the GHz frequency region. That is, by manipulating the various quantities, such as the radius and the number of the grains, and the constant magnetic field, the frequency domain for which the MPFG medium is transparent with LHM properties can be tuned.

Bibliography

- [1] S. Anantha Ramakrishna and Tomasz M. Grzegorzczuk, *Physics and Applications of Negative Index Materials*, CRC Press, New York (2009)
- [2] V.G. Veselago, *Sov. Phys. Usp.* 10, 509 (1968)
- [3] J.B. Pendry, A.J. Holden, W.J. Stewart, and I. Youngs, *Phys. Rev. Lett.* 76, 4773 (1996)
- [4] J.B. Pendry, A.J. Holden, D.J. Roberts, and W.J. Stewart, *IEEE Trans. Micr. Theory. Tech.* 47, 2075 (1999)
- [5] D.R. Smith, W.J. Padilla, D.C. Vier, S.C. Nemat-Nasser, and S. Schultz, *Phys. Rev. Lett.* 84, 4184 (2000)
- [6] Willie J. Padilla, Dimitri N. Basov, and David R. Smith, *Materials Today*, *Phys.* 9, 7-8 (2006)
- [7] R. Shelby, D.R. Smith, and S. Schultz, *Science* 292, 77 (2001)
- [8] C.G. Parazzoli, R.B. Greigor, K. Li, B.E.C. Koltenbah, and M. Tanielian, *Phys. Rev. Lett.* 90, 107401 (2003)
- [9] Jeo Pacheco, Jr, PhD dissertation, (**Theory and Application of Left-Handed Metamaterials**), (**MASSACHUSETTS INSTITUTE OF TECHNOLOGY**) (2004)

- [10] Shuang Zhang, Yong-Shik Park, Jensen Li, Xinchao Lu, Weili Zhang, and Xiang Zhang, Phys. Rev. Lett. 102, 023901 (2009)
- [11] Cheng-Wei Qui, Hai-Ying Yaom, Le-Wei Li, Said Zouhdi, and Tie-Soon Yeo, Phys. Rev B 75, 155120 (2007)
- [12] Victor Veselago, Leonid Braginsky, Valery Shklover, and Christian Hafner, J. Comput. Theor. Nanosci., Vol. 3, No. 2 (2006)
- [13] D.R. Smith, J.B. Pendry, M.C.K. Wiltshire, Science, 305 788-92 (2004)
- [14] Yongmin Liua and Xiang Zhang, Chem. Soc. Rev. 40, 24942507 (2011)
- [15] D.R. Smith and Norman Kroll, Phys. Rev. Lett. 85, 14 (2000)
- [16] R.A. Shelby, D.R. Smith, S.C. Nemat-Nasser, and S. Schultz, Appl. Phys. Lett. 78, 4 (2001)
- [17] Priy Dilipa Gauno Dessai, Master thesis, (**Influence of Chirality on the Electromagnetic Wave Propagation: Unbounded Media And Chirowaveguides**), (**Universidade Tecnica de Lisboa**) (2011)
- [18] Qiang Cheng and Tie Jun Cui, Phys. Rev B 73, 113104 (2006)
- [19] E. Plum, J. Zhou, J. Dong, V.A. Fedotov, T. Koschny, C.M. Soukoulis, and N.I. Zheludev, Phys. Rev B 79, 035407 (2009)
- [20] Jiangfeng Zhou, Jianfeng Dong, Bingnan Wang, Thomas Koschny, Maria Kafesaki, and Costas M. Soukoulis, Phys. Rev B 79, 121104(R) (2009)
- [21] V.M. Mal'nev, E.V. Martysh, and V.V. Pan'kiv, Ukr. J. Phys. 53, 8 (2008)
- [22] Belayneh Mesfin and V.N. Mal'nev, Phys. Plasmas 17, 112109 (2010)

- [23] Nicholson R. Dwight, *Introduction to Plasma Theory*, John Wiley and Sons, USA (1983)
- [24] John Howard, *Introduction to Plasma Physics*, Australia National University, Australia (2002)
- [25] L.D. Landau, E.M. Lifshitz, and L.P. Pitaevskii, *Electrodynamics of Continuous Media*, Pergamon, New York, 2nd edition (1984)